DEVELOPMENT OF ACTIVE PACKAGING MATERIALS FROM OLIVE MILL SOLID WASTE

PİRİNADAN AKTİF PAKETLEME MATERYALLERİNİN GELİŞTİRİLMESİ

KAMİL URGUN

PROF. DR. DİLEK SİVRİ ÖZAY

Supervisor

PROF. DR. BORA MAVİŞ

Co- Supervisors

Submitted to Graduate School of Science and Engineering of Hacettepe University as a Partial Fulfillment to the Requirements for the Award of the Degree of Master of Science in Food Engineering

2021

ABSTRACT

DEVELOPMENT OF ACTIVE PACKAGING MATERIALS FROM OLIVE MILL SOLID WASTE

Kamil URGUN

Master of Science, Department of Food Engineering

Supervisor: Prof. Dr. Dilek SİVRİ ÖZAY

Co- Supervisor: Prof. Dr. Bora MAVİŞ

June 2021, 45 pages

Polyvinyl alcohol (PVA)/Lignin composite nano fibers were fabricated from lignin obtained from olive mill solid waste (OMSW). Deep eutectic solvent (DES) prepared with choline chloride, glycerol, and aluminum chloride hexahydrate was used to extract lignin from OMSW. After the pretreatment cellulose rich (CRF) and lignin rich fractions (LRF) were obtained.

Effect of aluminum chloride hexahydrate concentration on DES pretreatment was investigated. Delignification ratio of choline chloride: glycereol: $AlCl_3.6H_2O$ (1:2:0.1 molar ratio) DES was higher (39.21 ± 0.35 %) as compared to other aluminum chloride hexahydrate concentrations. Highest antioxidant activity and purity of the LRF obtained after DES pretreatment was measured as 437.88 ± 7.14 (mmol TEAC/Kg sample) and 87.21 ± 0.36 %. Changes in structure of OMSW during pretreatment were also determined with FT-IR spectrometry. Peaks representing lignin (C=C stretching) were become sharper on spectra of LRF at the same time they were decreased on spectra of

CRF. Changes observed over hydrogen bonding related peaks as well. Cellulose related peaks (weak C-O stretching and C-H bending vibration of glucose unit) were increased on spectra of CRF and decreased on spectra of LRF.

LRF obtained from DES pretreatment used in production of defect free fine antioxidant poly(vinyl alcohol)/lignin composite nanofibers. Average diameter was 126 ± 17 nm and antioxidant activity was 85.84 ± 1.63 (mmol TEAC/Kg sample) at 4% lignin. Increasing lignin level resulted in higher antioxidant activity and samples containing 12% lignin had the highest antioxidant activity 131.15 ± 3.13 (mmol TEAC/Kg sample).

In order to reveal the effect of electrospinning on the antioxidant activity, PVA/lignin composite films were fabricated, and their antioxidant activity was compared with that of nanofibers. Fiber formation was increased antioxidant activity of films up to 68%.

Effect of electrospinning conditions like flow rate, distance and total solid concentration on fiber morphology determined by scanning electron microscopy (SEM). Optimum electrospinning conditions were 19.5 cm distance and 1.00 mL/hr flow rate.

As a result, antioxidant PVA/lignin composite nano fibers were fabricated from LRF produced from OMSW via DES pretreatment. To our knowledge there is no other study reported on production of nanofibers from LRF obtained from OMSW. Production of such fibers may used in food packaging area and this might led to valorization of a nature polluting waste.

Keywords: OMSW, PVA, Lignin, DES, Pretreatment, Nanofiber, Antioxidant activity, Electrospinning

ÖZET

PİRİNADAN AKTİF PAKETLEME MATERYALLERİNİN GELİŞTİRİLMESİ

Kamil URGUN

Yüksek Lisans, Gıda Mühendisliği Bölümü

Tez Danışmanı: Prof. Dr. Dilek SİVRİ ÖZAY

Eş Danışman: Prof. Dr. Bora MAVİŞ

Haziran 2021, 45 Sayfa

Pirinadan elde edilen lignin kullanılarak polyvinyl alkol (PVA)/lignin kompozit nano fiberler üretilmiştir. Pirinadan lignin; kolin klorür, gliserol ve alüminyum klorür hegzahidrat gibi derin ötektik çözücü (DÖÇ) kullanılarak ekstrakte edilmiştir. Bu önişlemden sonra pirinadan selülozca zengin kısım (SZK) ve lignince zengin kısım (LZK) elde edilmiştir.

DÖÇ işlemine alüminyum klorür hegzadihrat konsantrasyonunun etkisi araştırılmıştır. İçeriği kolin klorür: gliserol: $AlCl_3.6H_2O$ (1:2:0.1 molar oran) olan DÖÇ'ün delignifikasyon yüzdesi 39.21 ± 0.35'dur ve diğer alüminyum klorür hegzadihrat konsantrasyonlarından yüksek bulunmuştur. DÖÇ işlemi sırasında pirinanın yapısında

meydana gelen değişimler Fourier dönüşümlü kızıl ötesi spektroskopisi (FT-IR) ile belirlenmiştir. Lignine özgü C=C uzamasından kaynaklanan absorbsiyon bantları LZK'nın spektrasında artarken SZK'nın spektrasında azalmıştır. Hidrojen bağı nedeniyle gözlenen absorbsiyon bantlarında değişikler gözlenmiştir. SZK'nın spektrasında selüloz kaynaklı absorbsiyon bantlarında (C-O uzaması ve C-H bükülme titreşimi) artış gözlenmiştir aynı bantlar LZK'nın spektrasında küçülmüştür.

DÖÇ işlemi sonrasında üretilen LZK'ların antioksidan aktivitesi en çok 437.88 ± 7.14 (mmol TEAC/Kg örnek) olarak ve saflığı en çok %87.21 ± 0.36 olarak ölçülmüştür.

DÖÇ işlemi ile elde edilen LZK, kusursuz düzenli polivinil alkol/lignin kompozit nanofiber üretiminde kullanılmıştır. Lignin konsantrasyonu %4 olan PVA/lignin kompozit fiberlerinin ortalama çapı 126 ± 17 nm ve antioksidan aktivitesi 85.84 ± 1.63'tür (mmol TEAC/Kg örnek). Lignin seviyesinin artması antioksidan aktivitenin artması ile sonuçlanmış ve lignin miktarı %12 olan örnekler en yüksek antioksidan aktiviteyi göstermiştir (131.15 ± 3.13 mmol TEAC/Kg örnek).

Elektroeğitme işleminin antioksidan aktiviteye etkisini ortaya koymak için PVA/lignin kompozit filmler üretilmiştir ve filmlerin antioksidan aktiviteleri fiber ile karşılaştırılmıştır. Fiber üretimi antioksidan aktiviteyi %68'e kadar arttırmıştır.

Mesafe, akış hızı toplam katı konsantrasyonu gibi elektroeğirme koşullarının fiber morfolojisine etkisi taramalı elektron mikroskopisi ile belirlenmiştir. Optimum elektroeğirme koşulları 19.5 cm mesafe ve 1.00 mL/hr akış hızı olarak belirlenmiştir.

Sonuç olarak pirinadan DÖÇ ile elde edilen LZK kullanılarak PVA/lignin antioksidan kompozit nanofiberler üretilmiştir. Bildiğimiz kadarıyla, prinadan elde edilen LRF'den nanolif üretimi hakkında rapor edilmiş başka bir çalışma bulunmamaktadır. Üretilen fiberler gıda paketlemesinde kullanılabilir ve böylece doğayı kirleten bir atığın değerlendirilmesi gerçekleşmiş olur.

Anahtar Kelimeler: Pirina, PVA, Lignin, Elektroeğirme, Nanofiber, Antioksidan Aktivite, Önişleme

ACKNOWLEDGEMENTS

I would like to express my gratitude to my principle super visor Prof. Dr. Dilek Sivri Özay for her support throughout my studies. I also thank my co-supervisor Prof. Dr. Bora Maviş for his endless support, understanding and patience. It was a pleasure for me to study with him. I appreciate his mentorship both in laboratory and in my personal life.

I also thank Assoc. Prof. Dr. Fahriye Ceyda Dudak Şeker. During my studies whenever I had hard times to move on, she was ready to encourage me to push forward. Her help was very valuable for me. I also highly appreciate Prof. Dr. Deniz Çekmecelioğlu for his guidance.

The assistance provided by members of NANOMATIVE research group was greatly appreciated. Especially Mustafa Utku Yıldırım, he was best lab mate I can ask for. I really enjoyed the time we spent together.

I thank Mehmet Semercioğlu for providing olive mill solid waste.

I gratefully appreciate support of my family. They always supported and enlighten my path. Even though all of my decisions were not very realistic they keep supporting me. I can't express how lucky I am to have such a wonderful family.

METU SFFS, ODTÜ DKSK and METU Unicorns turned me to the person who I am today. I thank them to accept me while I grow up with them. I shared my best memories with them.

I thank my friends, Meltem Yıldırım, Yelda Zencir, Ecem Evrim Çelik, Seda Elikoğlu, Nurdan Ersöz, Merve Erman, Merve Çanga, Hafize Öz, Sergen Nazım Mısırlı, Büşra Akdeniz and Dilan Batur, Can Kaytaz for their friendship. Finally, I thank Cansu Bozkurt for loving and caring me more than I do.

CONTENTS

Page

LIST OF TABLES

LIST OF FIGURES

SYMBOLS AND ABBREVIATIONS

ABxTS	2,2′-Azino-bis(3-ethylbenzothiazoline-6-sulfonic acid)
AIL	Acid Insoluble Lignin
ANOVA	Analysis of variance
AOAC	Association of Official Agricultural Chemists
ASL	Acid Soluble Lignin
ATR	Attenuated Total Reflectance
CGAH	Choline Chloride:Glycerol:Aluminum chloride hexahydrate
CRF	Cellulose Rich Fragment
DES	Deep Eutectic Solvent
DI	Deionized Water
DMF	Dimethylformamide
DMSO	Dimethyl sulfoxide
DP	dimethyl sulfoxide/PVA
DPL	dimethyl sulfoxide/PVA/Lignin
FT-IR	Fourier Transform Infrared Spectroscopy
HBA	Hydrogen Bond Acceptor
HBD	Hydrogen Bond Donor
HMF	Hydroxymethylfurfural
IL	Ionic Liquid
LRF	Lignin Rich Fragment
NREL	National Renewable Energy Laboratory
OMSW	Olive Mill Solid Waste
OMWW	Olive Mill Wastewater
PCL	Polycaprolactone
PEO	Polyethylene oxide
PHA	Polyhydroxyalkonates
PVA	Polyvinyl alcohol
ROM	Rule of Mixture
SEM	Scanning Electron Microscopy
TEAC	Trolox Equivalent Antioxidant Capacity
UV	Ultra violet

1. INTRODUCTION

1.1. Lignocellulosic Biomass

Increasing energy consumption, limited fossil fuel stocks and environmental problems caused by fossil fuel consumption led to increase in usage of renewable resources as energy and chemical production. Biorefinery is the name given to the facilities which produce energy and valuable chemicals from renewable resources [1].

Lignocellulosic biomass [2, 3], food wastes [4-6], fish scale [7], and algae [8] are one of the most promising renewable resources used in biorefineries. World's annual lignocellulosic biomass production was estimated to be 181.5 billion tonnes [9]. There are three main polymers namely cellulose, hemicellulose and lignin which comprise majority of the solid part of lignocellulose. Their fraction varies depending on the source of biomass [10, 11].

Table 1: Cellulose, lignin and hemicellulose composition of some lignocellulosic materials [11]

Source	Composition %		
	Cellulose	Hemicellulose	Lignin
Corn cob	45	35	15
Rice straw	43	33	20
Wheat straw	30	50	15
Sisal	73	14	11
Flax	71	21	2
Hardwood	43-47	23-25	16-24
Cotton	95	2	1
Softwood	40-44	25-29	25-32

Cellulose is the most abundant biopolymer on Earth. Cellulose composition of lignocellulosic biomass changes between 95 % (cotton) to 30 % (wheat straw). β-D-glucopyranosyl units linked by β-(1→4) glycosidic bond are building blocks of cellulose (Figure 1). Hydrogen bonding between OH groups of glucose molecules increase stiffness of the cellulose giving it a semi crystalline fibrous structure [11, 12].

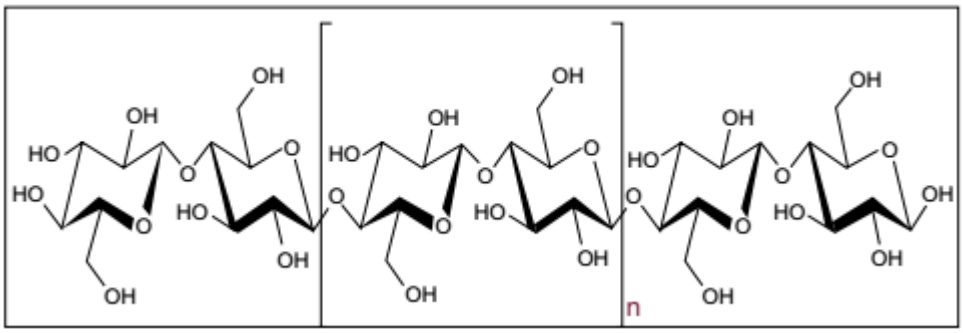

Figure 1:Molecular structure of cellulose [13]

Hemicellulose is the second most abundant carbohydrate in nature. It's structure changes depending on the source. Most common form of the hemicellulose is heterogeneous polymer which consists of pentoses (xylose and arabinose) and hexoses (mannose, galactose and glucose) linked to a β-(1→4) glycosidic bonded xylopyranose backbone. Hydroxyl groups of hemicellulose may be acetylated or may contain uronic acid side groups (Figure 2). Hemicellulose molecules are linked to cellulose fibrils by hydrogen bonds at cellulose surface and covalently bonded to lignin.

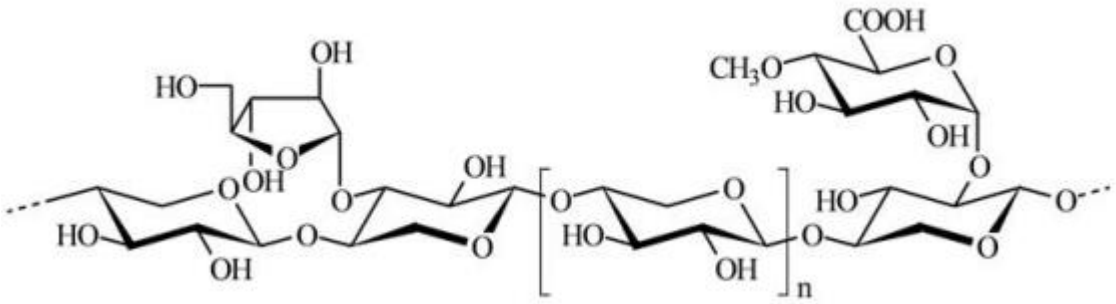

Figure 2: Structure of arabino-gluurono-xylan type hemicellulose [14]

Lignin is an amorphous, 3D structured, aromatic polymer. Sinapyl alcohol, coniferyl alcohol and paracoumaryl alcohol are 3 phenylpropene units which are major constituents of the polymer (Figure 3). They are covalently linked to hemicelluloses and in cell wall they fill in the place between hemicellulose and cellulose. It has a hydrophobic structure and provides lignocellulosic recalcitrance of the cell wall against degradation (Figure 4). It is hard to determine exact structure of native lignin. Structure changes significantly depending on the extraction method, source of the lignin, climate and nutrition of plant [11, 15].

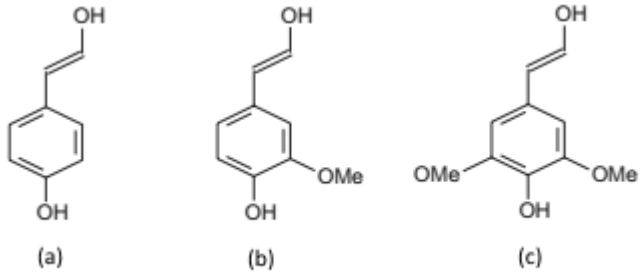

Figure 3: Structure of a:p-coumaryl alcohol, b: coniferyl alcohol, c: sinapyl alcohol [15]

1.2. Lignocellulose Pretreatment Methods

To produce value added products from lignocellulosic biomass, a process named pretreatment is applied to reduce recalcitrance and to separate lignin, hemicellulose and cellulose from each other. Currently alkali, acid, steam explosion, hydrothermal, ionic liquid and deep eutectic solvent (DES) based pretreatment methods are applied to lignocelluloses [16, 17] .

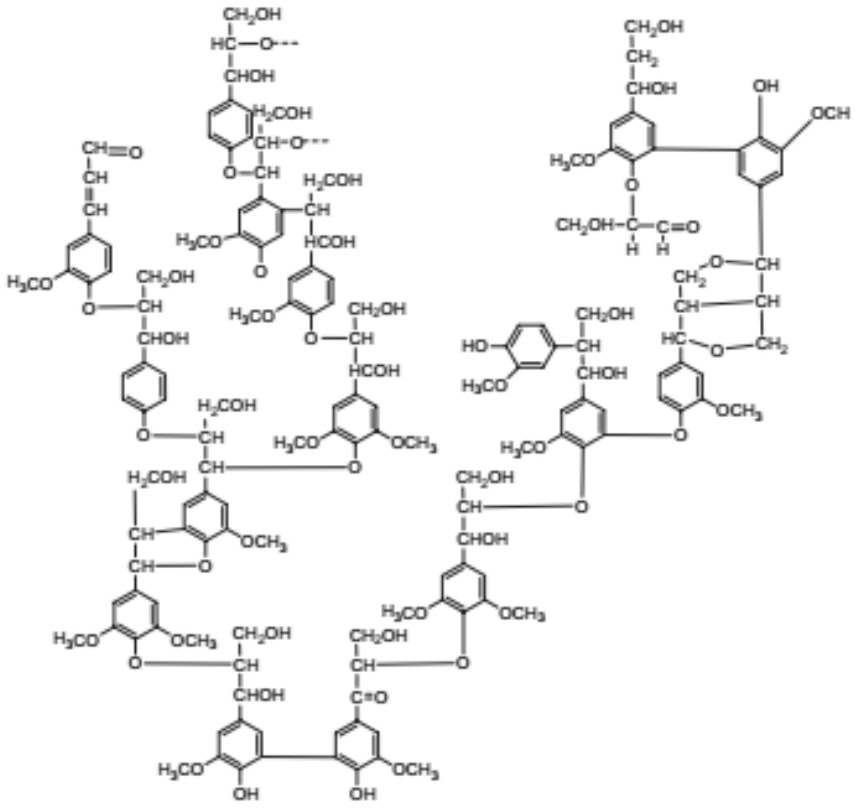

Figure 4: Softwood lignin structure as proposed by Adler [15]

1.3. Acid and Alkali Pretreatments

Pretreatment process applied at high pH generally solubilize lignin while do not affect hemicellulose and cellulose too much, thus result in high delignification. Lignin

solubilized in alkali solution named as black liquor and contains lignin and high concentration of metal ions (Na, K etc.). Lignin obtained with alkali pretreatment mostly used as heat source because high metal concentration of lignin prevents it's usage in further production processes. NaOH and KOH are mostly used in this kind of pretreatment [18].

Under acidic conditions biomass cooked under low pH. When lignocellulose heated under diluted acid (H_2SO_4, H_3PO_4, HCl etc.), hemicellulose degrades to pentoses and hexoses. If temperature and acid concentration increase, cellulose degrades to glucose and oligo saccharides as well. Under more acidic conditions hexose and pentose units degrades to toxic chemicals like hydroxymethylfurfural (HMF), levulinic acid and furfural. Temperatures between 100^oC – 210^oC and pretreatment times of minutes to several hours are commonly applied [19-23].

1.4. Steam Explosion and Hydrothermal Pretreatments

In steam explosion method lignocelluloses are heated with water in a high-pressure vessel and after a certain time, vessel is de-pressurized suddenly thus cell structure is disrupted. Time, pressure, lignocellulose particle size and de-pressurization speed are important parameters affecting efficiency of the process. Acetic acid, H_2SO_4 and SO_2 might be used as catalyst in this method [24-27]

Hydrothermal processes are similar to steam explosion in which lignocellulosic materials are heated with water under high temperature and pressure, but de-pressurization is not applied. Instead, higher temperature, pressure and time are applied. It's believed that auto ionization of water is responsible for cleavage of lignin-hemicellulose covalent bonds [28-30]

1.5. Organosolv (Organic Solvent Based) Pretreatment

A pretreatment process which uses an organic solvent to degrade and/or separate lignocellulosic biomass is named as organosolv pretreatment. A number of organic solvents are used in this method such as ethanol, formic acid, tethrahydrofuran, acetic acid, sulfuric acid, acetone and γ-valerolactone [31]. Organosolv processes like alkali treatment mostly dissolve lignin from lignocellulose. Depending on the used solvent properties and efficiency of the pretreatment changes significantly [32]. It is possible to obtain high purity lignin using organosolv method [33].

1.6. Ionic liquid Based Pretreatment

Ionic liquids (ILs) are molten salts depending on the ion source and they might be liquid even at room temperature [34, 35]. Since they can be formed between too many different anion and cation pairs, they show tunable properties like, density, viscosity and hydrophilicity [36, 37]. Their major advantages over other methods are their low volatility, flammability and high stability.

Aprotic ILs demonstrated some promising lignin dissolution abilities. Some of the ILs can successfully separate lignin from lignocellulose even at room temperature [31, 38, 39].

1.7. Deep Eutectic Solvent (DES) Based Pretreatment

DESs are mixture of two or more components, which have lower melting point than all components of the mixture. DES formed between choline chloride and urea with a molar ratio of 2:1 has a melting point of 12^{o}C while melting point of urea is 133^{o}C and melting point of the choline chloride is 302^{o}C [40]. Materials forming DES have strong hydrogen bonding between each other. One component acts as hydrogen bond donor (HBD) while the other acts as hydrogen bond acceptor (HBA).

Researchers focused on DESs due to their thermal stability, easy preparation process (generally mixed under 120^{o}C), low cost, nontoxicity, biodegradability, nonflammability and versatile use [41-43].

Starting from the day they were announced in 2003, DESs have been used in many different areas; as CO_2 absorbent [44], extraction solvent [45], metal oxide solvent [46], reaction catalyst [47], biodiesel purificator [48], as well as in organic molecule synthesis [49], nano material synthesis [41] and lignocellulose pretreatment [17, 41, 50].

DESs can efficiently pretreat lignocellulosic material including food wastes. According to Table 2, rice straw, corncob, garlic skin, green onion root and wheat straw were successfully pretreated with DES. It is possible to remove more than 90% of the lignin from the lignocellulosic biomass. As seen from the table, most of the DES systems depend on protic acids like formic acid, acetic acid and lactic acid. These acids have corrosive effects, and their wastes should be handled carefully. Under highly acidic conditions, cellulose and hemicellulose are degraded into HMF and furfural, which may not be desired for fermentation applications [51]

To improve applicability of DESs, polyols like ethylene glycol and glycerol were used as HBDs. Unfortunately delignification performance of these DESs was not very high. Researchers added Lewis acids likes aluminum chloride and iron(III) chloride to DESs formed with polyols as HBD. With this method greener and safer DESs have been produced [41, 52].

1.8. Olive Mill Solid Waste

Olive oil is produced from fruits of *Olea europaea* (olive tree). Annual olive oil production of the world is higher than 3379 million tons and olive oil consumption of the world is increasing [53]. It is estimated that current worldwide olive mill waste production is between 10-30 million m^3 [54]. According to International olive oil council, Turkey produced 423 million tons of olive oil in 2018-2019 season. This production led to approximately 1.25-3.75 million m^3 olive mill waste production [55].

Three different production methods are applied during olive oil production. Traditional pressing method, centrifugal methods using 2-phase decanters and 3-phase decanters. These systems produce two waste streams named olive mill wastewater (OMWW) and olive mill solid waste (OMSW). Two phase decanters create only one waste stream this waste stream is a mixture of both OMSW and OMWW [56]. Olive mill wastes have high free fatty acid and poly-phenolic compound contents and causes adverse effects like pollution of fresh water sources, inversely affects microbial respiration, soil contamination, foul smell and decreases dissolved oxygen level in water (Table 3).

Table 2: Deep eutectic solvent based biomass pretreatment methods and their delignification values

Type of DES	Biomass	Delignification %	Reference
Choline Chloride: Formic Acid	Poplar wood	76.4	[57]
Choline Chloride: Acetic Acid	Poplar wood	76.5	[57]
Choline Chloride: Lactic Acid	Poplar wood	73	[57]
Choline Chloride : Catechol	switchgrass	49	[58]
Choline Chloride : Vanilin	switchgrass	42.5	[58]
Choline Chloride : p-coumaric acid	switchgrass	60.8	[58]
Choline Chloride : glycerol + H_2O	switchgrass	63.84	[59]
Choline chloride : Glycerol	Garlic skin and green onion root	83.79 - 80.68	[52]
Choline chloride : Oxalic acid	Garlic skin and green onion root	68.83 - 63.98	[52]
Choline chloride : urea	Garlic skin and green onion root	75.50 - 79.31	[52]
Choline chloride: glycerol : aluminium chloride.6H2O	Garlic skin and green onion root	90.14 - 92.34	[52]
Choline chloride : Oxalic acid : aluminium chloride.6H_2O	Garlic skin and green onion root	83.03 - 85.78	[52]
Choline chloride : urea : aluminium chloride.6H_2O	Garlic skin and green onion root	87.66 - 88.73	[52]
Choline Chloride : Lactic acid	Wheat straw	81.5	[17]
Choline Chloride : Lactic Acid	Eucalyptus	93.2	[60]
Choline chloride: Glycerol: Iron(III) Chloride	Pennisetum energy grass	91	[41]
benzyltrimethylammonium chloride/lactic acid	Corncob	63.4	[61]
benzyltriethylammonium chloride /lactic acid (LA)	Corncob	56.5	[61]
guanidine hydrochloride : propylene glycol : p-toluenesulfonic acid	switchgrass	79.68	[62]
guanidine hydrochloride : ethylene glycol : p-toluenesulfonic acid	switchgrass	82.07	[62]
K_2CO_3 - Glycerol	Rice Straw	88.52	[63]

Wastes of olive oil production are generally dried in open ponds and used as fertilizer or burned to produce heat. A method to valorize OMSW and OMWW is needed to decrease these adverse effects on nature. Studies to decrease effects of OMSW can be categorized under three subgroups:

a) Decreasing waste by improving production systems and using 2 phase decanters
b) Recycling components of OMSW and OMWW
c) Detoxification of wastes

Table 3: Chemical compositions of live mill wastes. All data given as percentages.[56]

Property	Traditional press	3-phase decanter	2-phase decanter
Moisture	27.20	50.23	56.80
Oil & Fat	8.72	3.89	4.65
Protein	4.77	3.43	2.87
Cellulose	24.10	17.37	14.54
Lignin	14.10	10.21	8.54
Hemicellulose	11.00	7.92	6.63
Phenolic compounds	1.14	0.33	2.43

Physical methods (filtering, sedimentation, flotation, membrane process) applied on OMSW and OMWW efficiently decreased amount of adverse effects but alone these applications were not enough to solve problems caused by the waste [56].

Advanced oxidation processes and microbial digestion quite effectively detoxicate the waste, since these systems are expensive, they are not preferred and applied in the field [64]. To make waste management more efficient biorefinery concept is necessary to process olive mill wastes and produce valuable products from the waste. Olive mill wastes were used for production of polyhydroxyalkonates (PHAs), a biodegradable polyester [65]. Olive mill wastewater (OMWW) and olive mill solid waste (OMSW) contains high amount of functional compounds such as polyphenols. These compounds were extracted and used to produce functional products like antioxidant rich animal feeds [66], phenol rich food products with higher shelf life and nutrition value [67-70], antimicrobial and antioxidant packaging materials [71, 72] from OMWW or OMSW extracts but after the extraction huge amount of solid residue still remain as waste. Direct use of OMSW is still a challenge to overcome [73-76].

So far none of the systems proposed are applied on the field [77]. Olive oil producers keep polluting the nature with these wastes.

1.9. Electrospinning

Electrospinning is a fiber production method. In this method electric force is applied to a polymer solution and fiber with diameters up to nanometer scale are produced (Figure 5).

Electrospinning techniques enable to produce very thin fibers, thus increase surface area of the material, increases mechanical properties and functionalization of the compound. At the same time, it is quite easy to apply. These advantages made electrospinning a popular method to produce nanofibers [78].

So far electrospinning is used to produce nanofibers from more than 100 polymers such as; polystyrene, poly(vinyl alcohol), poly(vinyl chloride), poly(lactic acid), lignin, cellulose, collagen, dextran, chitin, chitosan and polyaniline [79]. Some of the lignin electrospinning studies were given at Table 4.

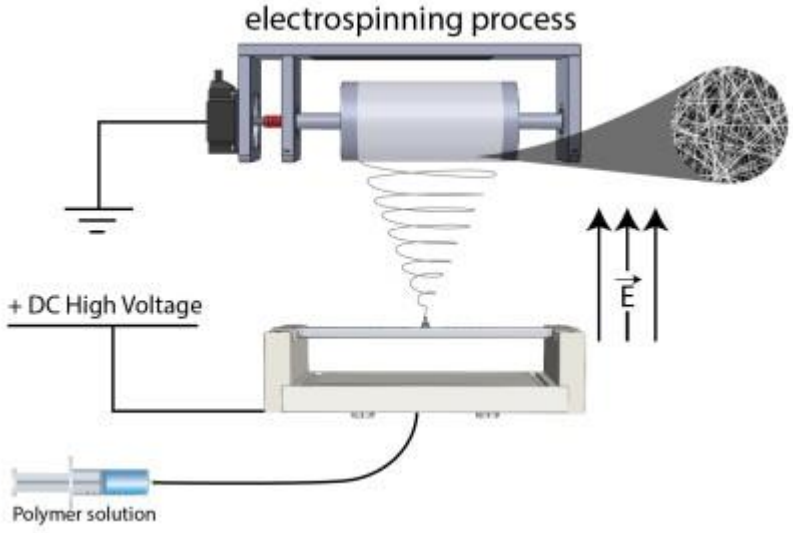

Figure 5:Electrospinning process [80]

These nano fibers had too many different properties. Some of the nanofibers had smart properties like; superhydrophilicity, superhydrophobicity, self-cleaning, shape memory, sensing and stimuli response. They are used in areas just as air purification, water treatment, selective adsorption from mixtures, enzyme immobilization, solar cells, rechargeable batteries, fuel cells, supercapacitors, tissue repair or regeneration and cancer research.

Lignin is also used to produce nanofibers via electrospinning method. Solvents like water, DMF, DMSO, acetic acid, formic acid and chloroform were used to dissolve lignin. In most of the cases researchers failed to form fibers from only lignin thus they fabricated lignin-based fibers with help of co-polymers. PVA, PEO and PCL are mostly used co-polymers.

Most of the literature focused on the production of carbon fibers from lignin-based nanofibers and application of them as anodes and supercapacitors. Some of the studies tried to use lignin-based fibers in water treatment applications. Only few of them suggested that lignin's antimicrobial, antioxidant and UV blocking properties could lead to an application in food packaging [65, 73-76].

In this study olive mill solid wastes (OMSW) obtained from 2-phase decanting system were pretreated with choline chloride: glycerol and aluminum chloride based ternary DES. After DES pretreatment, cellulose rich fragment (CRF) and lignin rich fragment (LRF) were obtained from OMSW. Effect of Lewis acid concentration to pretreatment efficiency of ternary DES system was evaluated and lignin purity, delignification ratio and antioxidant activity were determined. LRF obtained with the highest antioxidant activity used to produce polyvinylalcohol-ligin (PVA/lignin) nanofiber mats, which could be used as an active food packaging material. Along with fibers PVA/lignin composite films were also produced and their antioxidant activity were compared with PVA/lignin nanofibers. To our knowledge there is no other study reported on production of nanofibers from OMSW.

Table 4:Electrospun lignin based fibers, electrospinning solvent and application areas.

Lignin Source	Electrospinning polymer and solvent	Application	Reference
Lignin from flax sieve	PEO + lignin in DMF	carbon nanofiber	[81]
Organasolv lignin from rice husk	Lignin in chloroform : Acetone mixture	antioxidant fiber	[82]
Calcium lignosulfonate	PAN + lignin in DMSO	carbon nanofiber	[83]
Alkali lignin	lignin in water:glycerol mixture	carbon nanofiber	[84]
Alkali lignin low sulfonate	PVA + lignin in water	Supercapacitor	[85]
Alkali lignin low sulfonate	PVA + lignin in water	water treatment	[86]
Alkali lignin	PVA + lignin in water	water treatment	[87]
Lignin from sugarcane	PAN + lignin in DMSO:DMF mixture	carbon nanofiber	[88]
Alkali and kraft lignin	PAN + lignin in DMSO:DMF mixture	Supercapacitor	[89]
Low sulfonate alkali lignin	PVA + lignin in water	Supercapacitor	[90]
Low sulfonate alkali lignin	PCL + lignin in formic acid: acetic acid mixture	Antimicrobial fiber mat	[91]
Kraft lignin from eucalyptus	PEO + lignin in alkali water	Supercapacitor	[92]
Alkali lignin	PVA + lignin in water	Anode production	[93]
Kraft, organasolv and phosphoric acid lignin	PEO + lignin in DMF	Electrochemistry	[94]
Low sulfonate lignin	PVA + lignin in water	Anti-microbial and UV filter	[95]
Organasolv lignin	PAN + lignin in DMF	Thermoelectric properties	[96]
Kraft lignin	PEO + Soy protein + lignin in 0.1 M Acetonitrile solution	Mat production	[97]

PEO: poly ethylene oxide, PAN: Polyacrilonitrile, PVA: polyvinyl alcohol, PCL: poly caprolactone, DMSO: Dimethyl sulfuroxide, DMF:Dimethyformamid, TFA: trifluoro acetic acid.

2. MATERIALS AND METHODS

2.1. Materials

Olive mill solid waste (OMSW) obtained from a 2-phase decanter was kindly donated by Semercioğlu Zeytincilik (Edremit/Balıkesir). The OMSW was vacuum dried, milled using a laboratory blender (Arçelik, Turkey) and sieved with a 0.3 μm diameter sieve. The bottom of the sieve part has been stored at -18^{o}C until used.

Polyvinyl alcohol (PVA, mW 85.000 – 124,00, 89-87% hydrolyzed) and ABTS (2,2′-Azino-bis(3-ethylbenzothiazoline-6-sulfonic acid) were purchased from Sigma Aldrich. All other chemicals were analytical grade and used as obtained.

2.2. Characterization of Olive Mill Solid Waste

2.2.1. Moisture Content

Moisture content of the OMSW was measured according to AOAC method [98].

2.2.2. Protein Content

Kjeldahl method was used to determine protein content. About 1.5 g of sample was weighted into Kjeldahl digestion tubes, and 25 mL sulfuric acid (98 %) and 5 g catalyst (Mixture of Na_2SO_4 + $CuSO_4$ with 7:3 w/w ratio) were added. Sample was digested at 420^{o}C for 1 hour. NaOH solution (33 %, w/v) and boric acid solution (4 %. w/v) were used for distillation step. Few drops of Tashiri indicator were added as indicator. Samples were titrated with 0.1 N HCl [98]. Equation 2.1 was used to calculate protein concentration of OMSW samples. Conversion factor was 6.25. Results were reported as dry matter.

$$Protein\ Concentration = \frac{V_S - V_B * 1.4 * M * F}{m} \quad (2.1)$$

M = Molarity of HCl solution

m = Sample weight (g)

V_S = Volume of spent HCl for titration of sample

V_B = Volume of spent HCl for titration of blank

F = Conversion factor

2.2.3. Total Fat Content

Soxhlet method was used to determine fat content of the OMSW. Hexane was used as solvent and refluxed for 4 hours at 50^{o}C [98, 99].

2.2.4. Total Antioxidant Activity

Total antioxidant activity was measured by using ABTS solution as described by (Serpen et al. 2008) Briefly, 7 mmol/L ABTS (2,2′-azinobis(3-ethylbenzothiazoline-6-sulfonic acid) solution was reacted with 2.45 mmol/L potassium sulfate and diluted with 1:1 ethanol-deionized water mixture. This solution was used to determine antioxidant capacity of olive oil mill solid wastes (OMSW). If needed OMSW samples were diluted with cellulose. Cellulose was found to be inert against ABTS solution. Results were reported as mmol of Trolox equivalent antioxidant capacity (TEAC) [100].

2.2.5. Lignin Content

NREL procedure was employed for lignin content determination [101]. About 0.3 g sample was hydrolyzed with 3 mL 72% sulfuric acid at 30^{o}C for 1 hour. Later the solution diluted to 4% and autoclaved at 121^{o}C for 1 h. Sample was vacuum filtered through filtering crucible and filtrate was used to calculate acid soluble lignin (ASL) while filter cake was used to measure acid insoluble lignin (AIL) after samples cooled to room temperature.

Absorbance of filtrate was measured at 204 nm to determine ASL. Necessary dilutions were made with 4% sulfuric acid solution to have measurements between 0.7-1.0. Equation 2.2 was used to calculate ASL.

$$\%\, ASL = \frac{UVabs * Volume_f * Dilution\ rate}{\varepsilon * W_{sample} * pathlength} * 100 \qquad (2.2)$$

$UVabs = UV - vis\ absorbance\ recorded\ for\ sample$

$Volume_f = Volume\ of\ filtrate = 86.73\ mL$

$$Dilution\ rate = \frac{Volume\ of\ sample + Volume\ of\ diluting\ solvent}{Volume\ of\ sample}$$

$\varepsilon = absorptivity\ of\ the\ sample = 110$

$W_{sample} = Weight\ of\ the\ dry\ sample$

$pathlength = width\ of\ the\ uv - vis\ cell$

Crucibles were dried to a constant weight and recorded as $Weight_{crucible+sample}$. Crucibles were placed into a muffle furnace and kept at 575^{o}C for 8 hours. Later they were cooled down to room temperature in a desiccator. Their weight was recorded as $Weight_{crucible+ash.}$

AIL content was calculated with equation 2.3.

$$\% AIL = \frac{Weight_{Crucible+sample} - Weight_{Crucible+ash}}{W_{sample}} * 100 \quad (2.3)$$

$$W_{sample} = Weight\ of\ the\ dry\ sample$$

Total lignin content was expressed as sum of AIL and ASL.

2.3. DES Preparation

Deep eutectic solvents (DES) were prepared by mixing HBDs with HBAs at 80^{o}C. First choline chloride (ChCl) was mixed with glycerol (gly) to form Chcl:gly DES. After 1-hour $AlCl_3.6H_2O$ was added and mixed until homogeneous liquid was formed [102]. Four different DES were formed with different $AlCl_3.6H_2O$ (0.1, 0.2, 0.3, 0.4 molar ratios) concentrations. DESs were named as CGAH-1, CGAH-2, CGAH-3 and CGAH-4 where numbers represent molar ratio of $AlCl_3.6H_2O$ of DES. CGAH-1 for Choline Chloride: Glycerol:$AlCl_3.6H_2O$ DES was formed with molar ratios of (1:2:0.1). Other DESs were named in a similar way.

2.4. DES Pretreatment

DES and OMSW were mixed at 110^{o}C for 4 hours. Solid to solvent ratio was 10% (w/w). After 4 hours the mixture was cooled to room temperature. Later 45 mL 1:1 (v/v) acetone water mixture was added to mixture and magnetic stirrer was used to mix solvent at 250 rpm and room temperature. After mixture was centrifuged (Kubota 7780, Japan) at 20000 g for 10 minutes and supernatant was filtered through cellulose filter paper the precipitate was mixed with 45 mL acetone and centrifuged and filtered 2 more times. Filter cake was obtained after 3 filtrations and dried at 80^{o}C in a vacuum oven. The dried filter cake was named as cellulose rich fragment and used to determine delignification ratio.

Filtrates from first two filtrations were combined and acetone was rotavaporated at 55^{o}C for 30 minutes. Deionized water (DI) was added to the remaining mixture to total volume of 250 mL and mixture was centrifuged at 20000 g for 10 minutes. Supernatant was taken from the centrifuge bottle and 250 mL (DI) was added to bottle and

centrifuged one more time. Last step was repeated two times. The obtained precipitate was named as lignin rich fraction (LRF) and dried under vacuum oven and stored at -18^{o}C.

2.5. Delignification Ratio

Delignification ratio was calculated using equation 2.4.

$$Delignification\ Ratio = \frac{(L_1 - L_2)}{L_2} * 100 \quad (2.4)$$

L_2 = Lignin content of OMSW before pretreatment

L_1 = Lignin content of cellulose rich fraction

2.6. Lignin Extraction from LRF

About 0.15 g LRF was mixed with 5 g DMSO and stirred at 80^{0}C for 4 hours. The mixture was then filtrated through pre dried and weighted filter paper.

The following equation was used to calculate the dissolved amount of lignin in DMSO.

$$EL = 0.15 - (m_1 - m_2)$$

m_1 = Constant weight of filter paper + Filter cake (g)

m_2= Constant weight of filter paper (g)

EL = Amount of extracted lignin (g)

The lignin extracts were evaporated to 5mL volume and used to prepare electrospinning solutions.

2.7. Electrospinning Solution Preparation

In this study dimethyl sulfoxide/PVA (DP) and dimethyl sulfoxide/PVA/Lignin solutions were prepared for electrospinning. DP solutions were named as DP_{xy} where xy stands for PVA concentration of solution. DPL solutions were named as $DPL_{ab\text{-}cd,}$ where ab represents total solid percentage of solution while cd is lignin percentage of solids in solution (100*lignin/PVA).

To prepare DP solutions PVA and DMSO were mixed at 80^{o}C for 2 hours with a magnetic stirrer working at 100 rpm.

The lignin extracts obtained before were used to prepare DPL solvents. Precalculated amount of DMSO and PVA were added to extracts and mixed at 80^{o}C for 2 hours.

2.8. Electrospinning

Direct current voltage supplier (max 30 kV) combined with a syringe pump was used for electrospinning. Electrospinning solutions were filled into a 10 mL plastic syringe with a 15 G needle. Needle was covered with positively charged auxiliary electrode and placed horizontally over a metal plate covered with aluminum foil. Spined fibers were carefully peeled from foil.

A total of 12 different DMSO/PVA/lignin solutions were prepared for electrospinning process and concentrations of the solutions are given in Table 5.

Table 5:List of electrospinned solutions

Sample	DMSO (w%)	PVA (w%)	Lignin (w%)	Lignin percentage of solid
DP-10	90.00	10.00	-	-
DP-12	88.00	12.00	-	-
DP-14	86.00	14.00	-	-
DP-16	84.00	16.00	-	-
DP-18	82.00	18.00	-	-
DP-20	80.00	20.00	-	-
DPL-16-4	84.00	15.39	0.62	4.00
DPL-16-8	84.00	14.81	1.19	8.00
DPL-16-12	84.00	14.29	1.71	12.00
DPL-18-4	81.98	17.33	0.69	4.00
DPL-18-8	82.00	16.66	1.33	8.00
DPL-18-12	82.00	16.07	1.93	12.00

DP-aa: DMSO/PVA-weight-percent of pva in solution, DPL-bb-cc: DMSO/PVA/Lignin-weight percent of total solids in solution-lignin percentage of solids

2.9. Preparation of PVA/Lignin Films

PVA/Lignin films were prepared via solution casting method. The same solutions used for electrospinning process were used to produce PVA/Lignin films. After solutions cast on the glass plate, they were evaporated in drying oven for 4 hours at 80^{o}C. Three different films were produced with different lignin concentrations. PL-4, PL-8 and PL-12 for PVA/lignin films with lignin concentration of 4, 8 and 12%.

2.10. Fourier Transform Infrared Spectroscopy (FT-IR) Analysis

Thermo scientific Nicolet 6700 (USA) equipped with ATR (Attenuated Total Reflectance) sampling accessory was used to record FT-IR spectra of the samples. Analyses were conducted as 64 accumulation scans in the range of 650 to 4000 cm^{-1} with 4 cm^{-1} resolution.

2.11. Morphological Analysis (SEM)

Morphological structure and fiber diameters of the nanofibers were imaged by scanning electron microscopy (SEM) (FEI Quanta 200F) available at Bilkent University UNAM facilities (Ankara). Fiber samples placed over a metal stab, which was covered with carbon tape. Stab was coated with gold palladium (10 nm) and their SEM images were taken. Diameters of the fibers were calculated from SEM images for this purpose Image J software (Maryland, USA) were used. Diameters of at least 50 fibers from each sample were used in calculation.

2.12. Statistical Analysis

ANOVA (Analysis of variance) was used to determine significant differences in results. If any significant differences found, Tukey's multiple comparison test was applied for differences ($p<0.05$). Analyses were conducted using IBM SPSS software version 23.0 (SPSS Inc., Chicago, IL). In this study, the data were reported as average of two duplicate with standard deviation.

3. RESULTS AND DISCUSSION

3.1. Chemical Composition of Olive Mill Solid Waste

Moisture, protein, total fat, lignin contents and antioxidant activity of the OMSW were measured and results are shown in Table 6.

*Table 6:Chemical composition of olive mill solid waste**

Compound	Composition (w)
Moisture	78.64 ± 0.56
Fat	10.56 ± 0.02
Protein	7.41 ± 0.10
Acid Soluble Lignin	8.50 ± 0.24
Acid Insoluble Lignin	23.44 ± 0.45
Total Lignin	31.95 ± 0.23

*Compositions (except moisture content) reported on dry basis

Two phase decanters consume less water than other systems but OMSW produced from two phase decanters tended to have higher moisture content [56]. Indeed, moisture content of the OMSW changes considerably depending on the production system. Moisture content of OMSW sample used in this study was 78.64 %. Most of the reported moisture contents for OMSW ranged between 50–75 % [103]. Fat, protein and lignin contents of the OMSW sample were similar to values reported before [56, 72, 99, 103, 104]

3.2. Effect of Lewis Acid Concentration on OMSW Pretreatment

Effect of Lewis's acid concentration of choline chloride, glycerol and $AlCl_3.6H_2O$ DES on OMSW pretreatment were evaluated. Effectiveness of DES pretreatment was calculated with delignification ratio of OMSW and purity of the obtained lignin rich fragment (LRF). Antioxidant activity of LRF used in production of nanofibers was measured. Delignification ratio, lignin purity and antioxidant activities of the samples are given in Table 7.

Delignification ratios of the CGAH-1 and CGAH-2 samples were 39.21 % and 37.72 % respectively. Further increase of Lewis acid concentration caused a decrease in delignification power of the DESs significantly ($p<0.05$). Delignified ratio of CGAH-3 sample was 24.86% of the available lignin. Delignifying ratio of CGAH-4 was 12.60 % due to less powerful DES.

Lignin purity of all DES systems was higher than 80%. Although it has a lower delignification ratio, CGAH-3 produced the purest lignin rich fraction with purity of 87.21 %. Other lignin rich fractions had close purity values of 84.84 %, 83.26 % and 83.98 % for CGAH-1, CGAH-2, CGAH-4 samples, respectively. CGAH-2 sample had the highest antioxidant activity followed by CGAH-1, CGAH-3 and CGAH-4 samples (Table 7).

Haipeng et al (2018) pretreated poplar wood samples with chloline chloride:glycerol and $AlCl_3.6H_2O$ based DESs. They used five different $AlCl_3.6H_2O$ concentrations to understand the effect of Lewis acid concentration on pretreatment efficiency. They find out that delignification value of given DES system reached above 95% and purity of the lignin was higher than 90%. Increasing $AlCl_3.6H_2O$ molar ratio of DES beyond 0.28 decreases delignification ratio as found out in our study as well [105].

Lignocellulosic recalcitrance is affected by lignin content, hemicellulose structure, and acetyl groups connected to hemicellulose and proteins. Lignin provides chemical, microbiological and physical protection to plant cell wall. It prevents cellulase enzyme to access cellulose, deactivates some enzymes by ligin derived compounds and provides mechanical strength to plant tissues. Lignin content and properties of lignin changes depending on variety of the plant [106].

Lignin purity and delignification percent of the pretreatment method vary depending on the recalcitrance and pretreatment method. Delignification of switch grass with different DES ranged from 28%-70% [58]. Similar range was observed for delignification of wheat straw with DES 32%-83% [17]. Application of same DES pretreatment to different lignocellulosic biomass might affect the result as well. In hardwood and softwood samples pretreated with the same DES lignin yields measured as 78% and 58% respectively [107].

Ratio of building units (*p-coumaryl, coniferyl and sinapyl alcohol*) of lignin to each other effects lignocellulosic recalcitrance. OMSW lignin has sinapyl alcohol units dominantly [56]. There are studies indicating a positive correlation between sinapyl/coniferyl unit ratio and lignocellulosic recalcitrance [108, 109]. According to our knowledge there is no other study, which applied DES for lignin extraction from

OMSW. Structural difference of OMSW might explain the lower delignification values obtained in this study. Multisite Cl^- ion sourced from $AlCl_3.6H_2O$ is able to form strong hydrogen bonds with OH groups and competes with OH groups of lignin to break hydrogen bonding network of lignocellulose. Acidolysis of the weak (C-O) ether bond of the lignin is tended to be cleaved and hydrated and protonated to form phenol groups. Increase in syringyl and guaiacyl type phenolic -OH groups increase antioxidant activity of the lignin rich fragment. In another study, syringyl phenolic -OH and total phenolic -OH content of pretreated lignin were found to be related to antioxidant activity of lignin samples [110]. Antioxidant activity of LRF is not affected by lignin content or purity alone. Amount and composition of -OH groups affect antioxidant activity of LRF. This finding supports that even though CGAH-2 does not produce purest lignin it might exhibit highest antioxidant activity.

*Table 7:Effectiveness of DES pretreatment methods**

Sample	Delignification Ratio (%)	Lignin Purity (%)	Antioxidant Activity of LRF (mmol TEAC/kg sample)
CGAH-1	39.21 ± 0.35^a	84.84 ± 0.40^b	335.88 ± 10.29^b
CGAH-2	37.72 ± 0.63^a	83.26 ± 0.79^b	437.88 ± 7.14^a
CGAH-3	24.86 ± 2.20^b	87.21 ± 0.36^a	322.25 ± 6.48^c
CGAH-4	12.60 ± 0.80^c	83.98 ± 0.52^b	150.44 ± 1.70^d

*Different letters under same column represents significant difference ($p<0.05$) between samples.

CGAH-1 and CGAH-2 delignified higher ratios than CGAH-3 and CGAH-4. LRF obtained from pretreatment with CGAH-2 had highest antioxidant activity. Amount of lignin produced and amount of OMSW valorized at the end of this procedure strongly depend on delignification ratio. At the same time working with more antioxidant LRF increases potential antioxidant activity of the final product. CGAH-2 was chosen to characterize and produce nanofibers.

3.3. Attenuated Total Reflectance Fourier Transform Infrared Spectroscopy (ATR-FTIR)

DES pretreatments resulted in changes in chemical structure and functional groups of the lignocellulosic materials. These changes were detected via ATR-FTIR. Spectra of OMSW, pure cellulose, LRF and CRF were obtained after CGAH-2 pretreatment given in Figure 6.

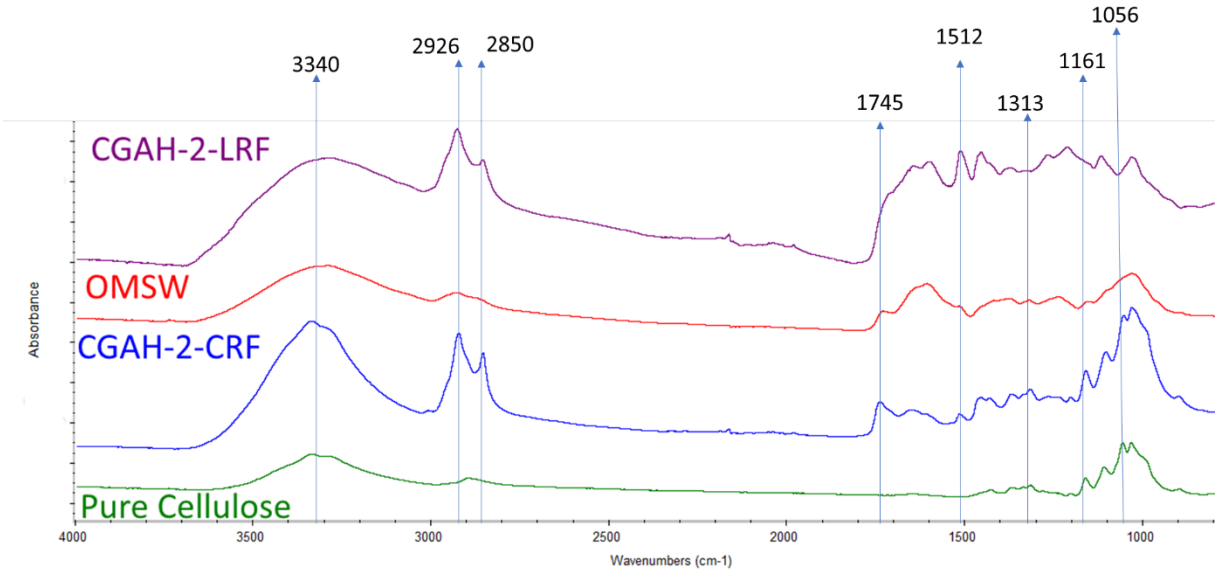

Figure 6:FT-IR spectra of samples. CGAH-2-LRF: Lignin rich fraction of OMSW after pretreatment with DES CGAH-2, OMSW: Olive mill solid waste before pretreatment, CGAH-2-CRF: Cellulose rich fraction of OMSW after pretreatment with DES CGAH-2.

Intense and broad peak between 3200-3400 cm^{-1} belongs to -O-H stretching vibration motion of the hydrogen bonded hydroxyl groups. All samples demonstrate this peak. Peaks at 2850 and 2926 cm^{-1} represent asymmetric and symmetric -C-H stretching band in aliphatic chains, $-CH_2$ groups of hemicellulose, cellulose and lignin. After pretreatment, those peaks become sharper, revealing that samples had different -OH and $-CH_2$ group structures [104].

The 1745 cm^{-1} peak attributed to C=O stretching of hemicellulose. Pretreatment makes it more silent and peak turns into a shoulder on LRF. Same peak's intensity increases on CRF indicating that pretreatment disrupted hemicellulose–lignin covalent bonds but hemicellulose–cellulose connections preserved [52].

C=C very strong stretching of aromatic skeletal observed at 1512 cm^{-1}. Increasing lignin concentration made that peak more intense [111]. 1056, 1161 and 1313 cm^{-1} peaks belong to cellulose unit all those peaks become sharper and more intense on CFR [112].

As a result, DES pretreatment increased asymmetric and symmetric -C-H stretching of both CRF and LRF. After the pretreatment intensity of lignin specific peaks of LRF get stronger, while hemicellulose and cellulose based peaks get weaker. Spectra of CRF was similar to spectra of pure cellulose. Effect of hemicellulose and lignin was clearly seen. This supports analytical experiment results given in Table 7. DES pretreatment produced two fractions one is rich in lignin, while other is rich in cellulose.

Table 8: FT-IR absorption bands of related peaks

Absorption band location (cm^{-1})	Type of vibration	Reference
3500 - 3100	Stretching vibrations of OH groups take place in hydrogen bonding	[57]
2925	Vibrations of asymmetric C-H stretching band	[104]
2855	Vibrations of symmetric C-H stretching band	[104]
1742-1710	C=O stretching in carbonyl esters and carboxylic groups	[104]
1511	very strong aromatic ring stretch C=C	[57, 113]
1319	weak C-O stretching	[113]
1160	C-H ring in plane bending vibration of glucose unit	[112]
1061	C-O-C asymmetric stretching vibration of cellulose	[52]

3.4. Surface Morphology of PVA Nanofibers

Six different DMSO/PVA solutions were prepared and electrospun at several voltage and distances to produce PVA nanofibers. SEM images of fibers are given in Figure 7. DP-10 solution was electrospun at 13 kV and resulted in few fibers surrounded with beads and droplets. Fiber formation of DP-12 was better than DP-10 but sample was contained too many beads. DP-14 and DP-16 were electrospun at the range of different voltages (15, 20 and 25 kV) and distances (11.0 and 19.5 cm). Most of the combinations resulted in regular fibers with few beads and some of them was defect free fibers. DP-18 and DP-20 produced most uniform fibers.

Diameters of only defect free fibers were calculated. Diameters of DP-10, DP-12, DP-14 were not calculated because these samples had some fine fibers along with large, beaded regions. Calculated diameters of PVA fibers and their spinning conditions are summarized in Table 8. Finest fibers were obtained from DP-18 with diameter 137 nm. Fibers of DP-16 and DP-20 had diameter of 204 and 296 nm respectively. These results were agreement in the relevant literature. Increasing PVA concentration decreases

surface tension of PVA solution, and this is the reason why fiber morphology improves up to a crucial concentration. Above this concentration PVA solutions starts to form thicker fibers [114]. Increasing PVA concentration improved fiber quality drastically. With higher PVA concentration, number of beads and irregularity of the fibers decreased. Concentrations above 18% PVA resulted in fibers without any beads. Since DP-16 and DP-18 were better than the other DMSO/PVA solutions, 16% and 18% solutions were used to form PVA/lignin composite fibers.

Table 9: Diameters of PVA fibers and spinning parameters.

Sample	Diameter (nm)	Voltage (kV)	Distance(cm)	Flowrate (mL/hr)
DP-16	204 ± 56	28.00	19.50	1.00
DP-18	137 ± 22	24.00	19.50	0.50
DP-20	296 ± 51	25.00	25.50	0.25

3.5. Surface Morphology of PVA/Lignin Composite Nanofibers

Six different PVA/Lignin composite fibers were produced. Samples containing 4% lignin (DPL-16-4 and DPL-18-4) managed to form defect free fibers. All other samples possessed sprayed solution residues on fibers. Optic images of fibers are given in Figure 8. SEM images (given in Figure 9) of DPL fibers demonstrated that DPL-16-4 and DPL-18-4 were defect free uniform fiber mats. DPL-16-8, DPL-16-12, DPL-18-8 and DPL-18-12 samples had beads and defects caused by solvent left in fiber mat after electrospinning. Fiber diameters (Table 10) ranged between 220 nm and 126 nm.

Addition of 4 and 8 % lignin to 16% total solid containing electrospinning solution improved fiber morphology. Neat PVA fiber was formed with 16% total solid in DMSO had unevaporated DMSO regions (figure 7-E), on the other hand DPL-16-4 fibers had no defect. Fiber diameter also decreased with addition of PVA. Strong hydrogen bonding between lignin and PVA might lead to easier evaporation of DMSO from the polymers and improve the fiber morphology [87].

*Table 10: Diameter and spinning conditions of PVA/Lignin composite nanofibers**

Sample	Diameter (nm)	Flow rate (ml/hr)	Voltage (kV)	Distance (cm)
DPL-16-4	149 ± 21^{b}	0.10	28	25.5
DPL-16-8	126 ± 17^{c}	0.50	28	19.5
DPL-16-12	$154 \pm 34^{a,e}$	0.10	28	19.5
DPL-18-4	154 ± 19^{a}	1.00	25	25.5
DPL-18-8	$220 \pm 28^{a,e,f}$	0.25	22	25.5
DPL-18-12	$155 \pm 18^{a,f}$	0.10	28	25.5

*Different letters within same column represents significant difference ($p<0.05$) between samples.

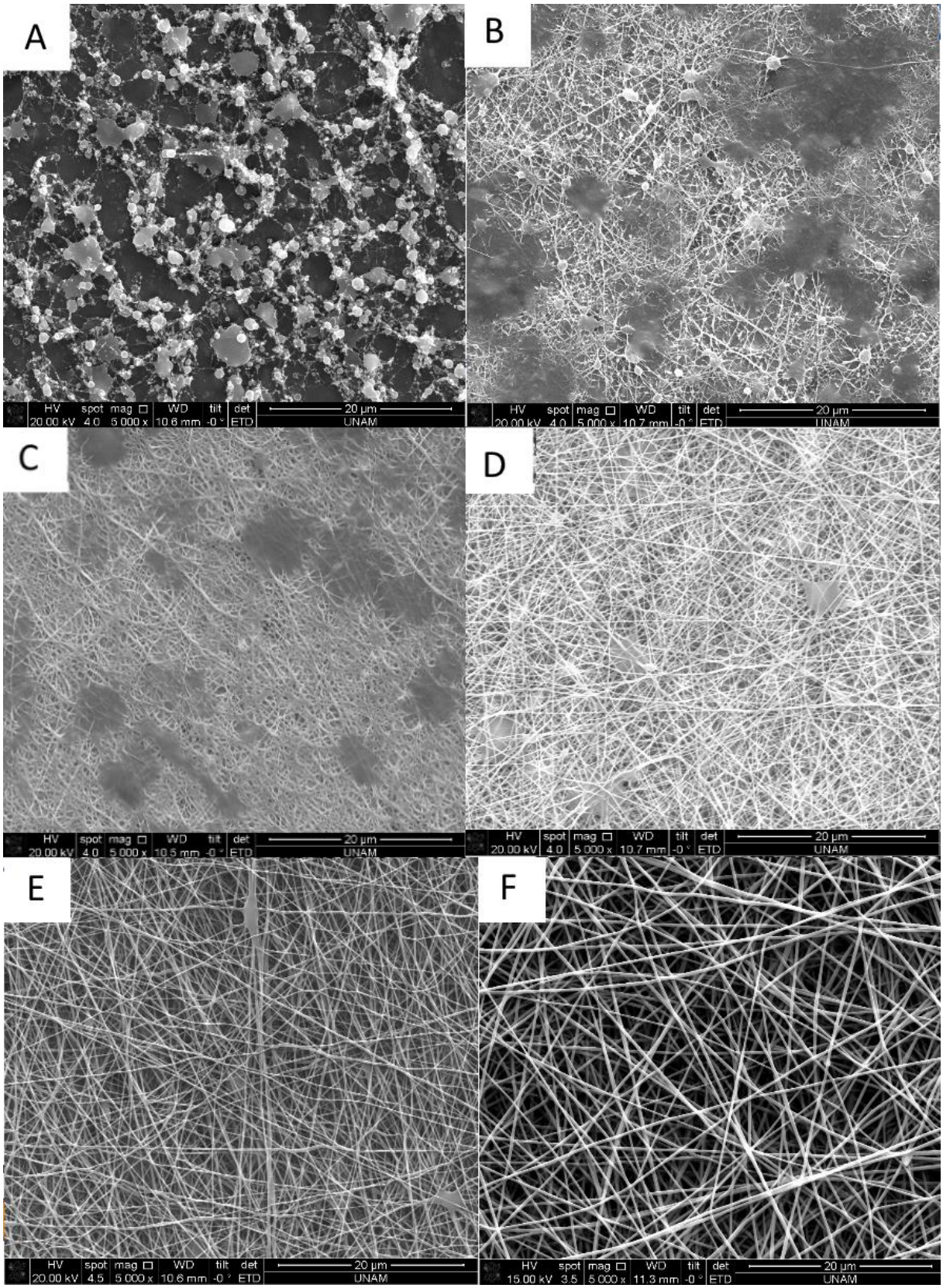

Figure 7: SEM images of PVA Fibers. A: DP-10, B: DP-12, C: DP-14, D: DP-16, E: DP-18, F: DP-20

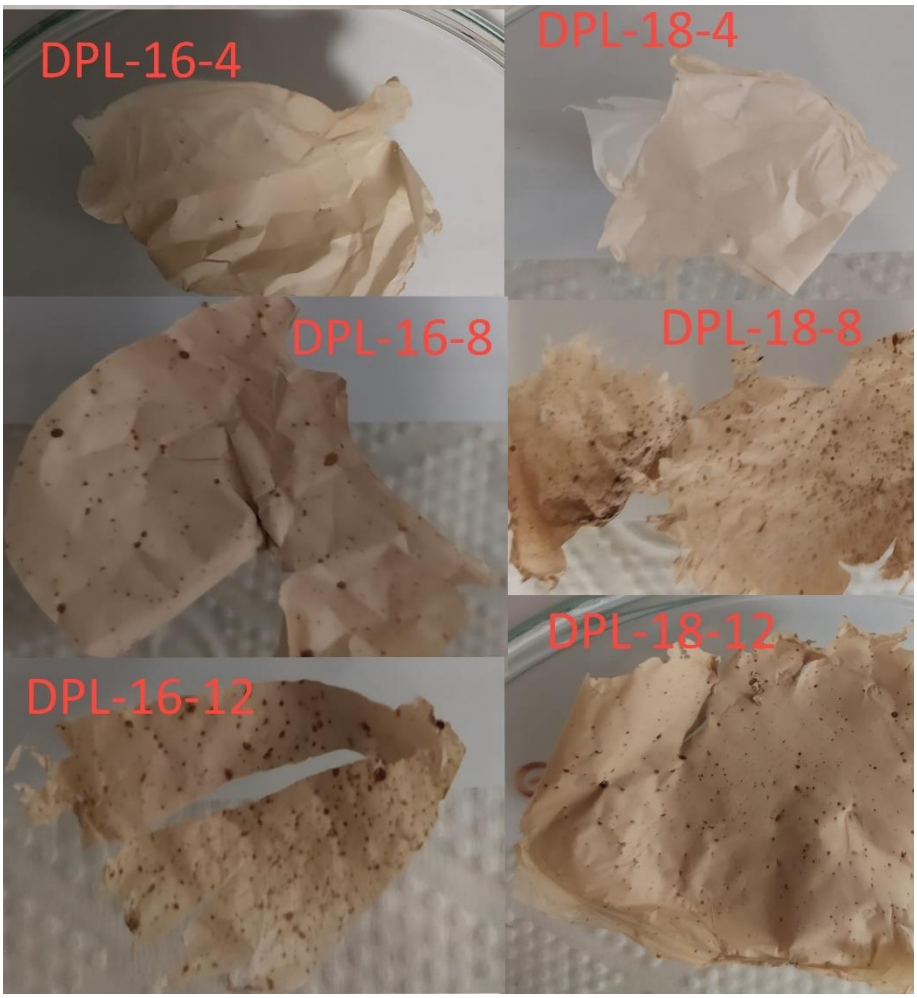

Figure 8: Optic images of DPL fibers

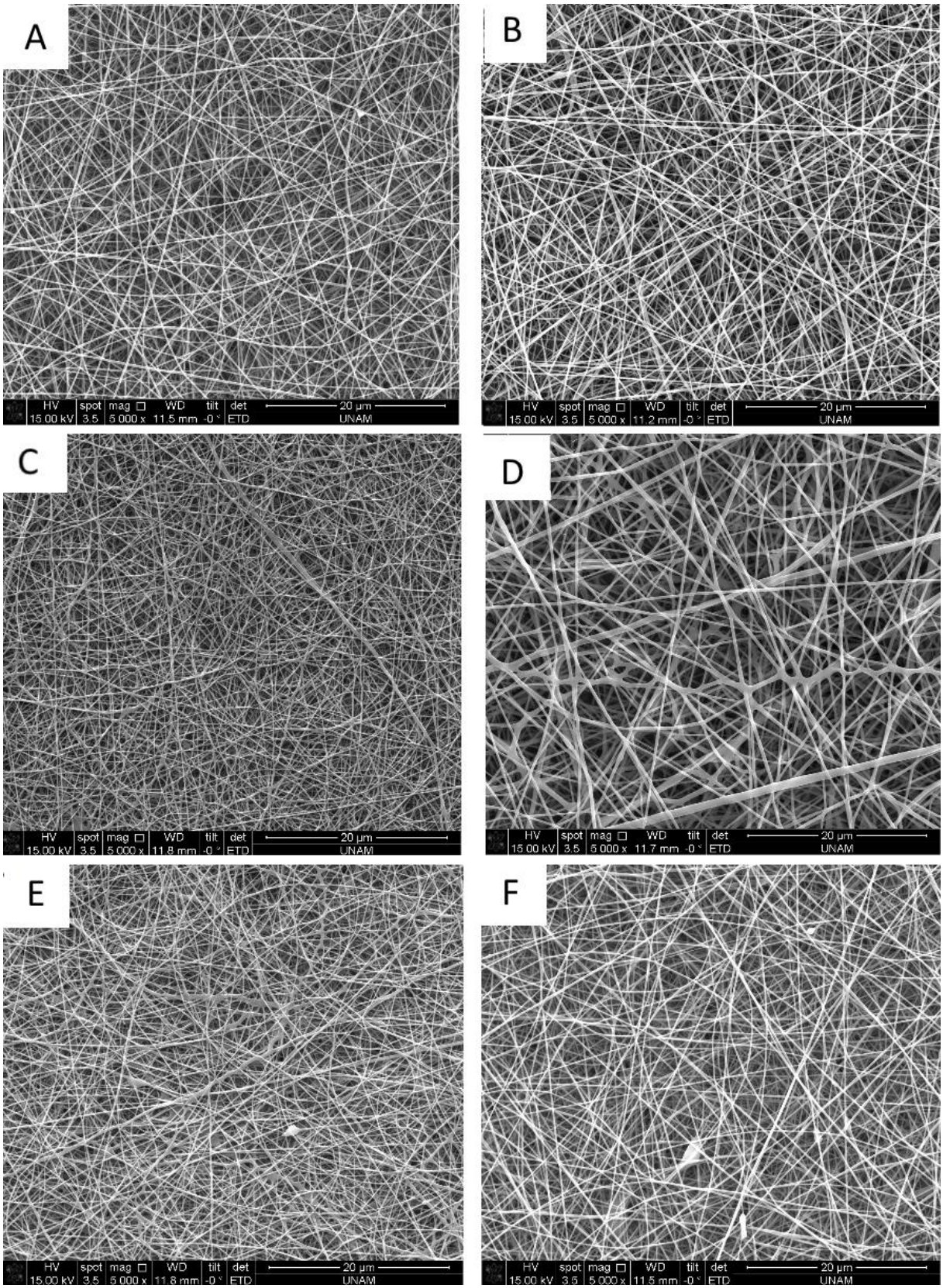

Figure 9: SEM images of DPL fibers. A: DPL-16-4, B: DPL-18-4, C: DPL-16-8, D: DPL-18-8, E: DPL-16-12, F: DPL-18-12

3.6. Effect of Flow Rate on PVA/Lignin Fiber Diameter

To determine the effect of flow rate on fiber diameter of PVA/Lignin composite fibers, the DPL-18-4 sample was electrospun with three different flow rates (0.10, 0.50 and 1.00 mL/hr) while distance and voltage kept constant. Experimental conditions and fiber diameters are shown in Table 11. Samples were named according to their flowrates. DPL-18-4 was electrospun at 0.10 mL/hr and represented by DPL-18-4-0.10 other two samples were named as DPL-18-4-0.50 and DPL-18-4-1.00 similarly. SEM images of the fibers are given in Figure 10.

*Table 11: Experimental conditions and fiber diameters of DPL-18-4 solution at different flow rates**

Sample	Diameter (nm)	Flow rate (ml/hr)	Voltage (kV)	Distance (cm)
DPL-18-4-0.10	183 ± 30^{a}	0.10	25	25.5
DPL-18-4-0.50	161 ± 27^{b}	0.50	25	25.5
DPL-18-4-1.00	154 ± 19^{c}	1.00	25	25.5

*Different letters within same column represents significant difference ($p<0.05$) between samples.

Results revealed that flow rate effects diameter of the electrospun fibers. Increasing flow rate up to a critical limit improved fiber morphology. After that point fibers had defects like bead and high diameter was observed. If flow rate was less than the critical point, polymer jet started to emerge directly from inside of the needle and continuously are replaced between cone jets and inside of the needle jets [115]. This phenomenon leads to increase in diameter and production of fibers with wide diameter range [116]. For DPL-18-4 solution increasing flow rate from 0.10 ml/hr to 1.00 ml/hr resulted in formation of smaller and more uniform fibers. For DMSO/PVA/Lignin system the critical point for electrospinning was close to 1.00 ml/hr.

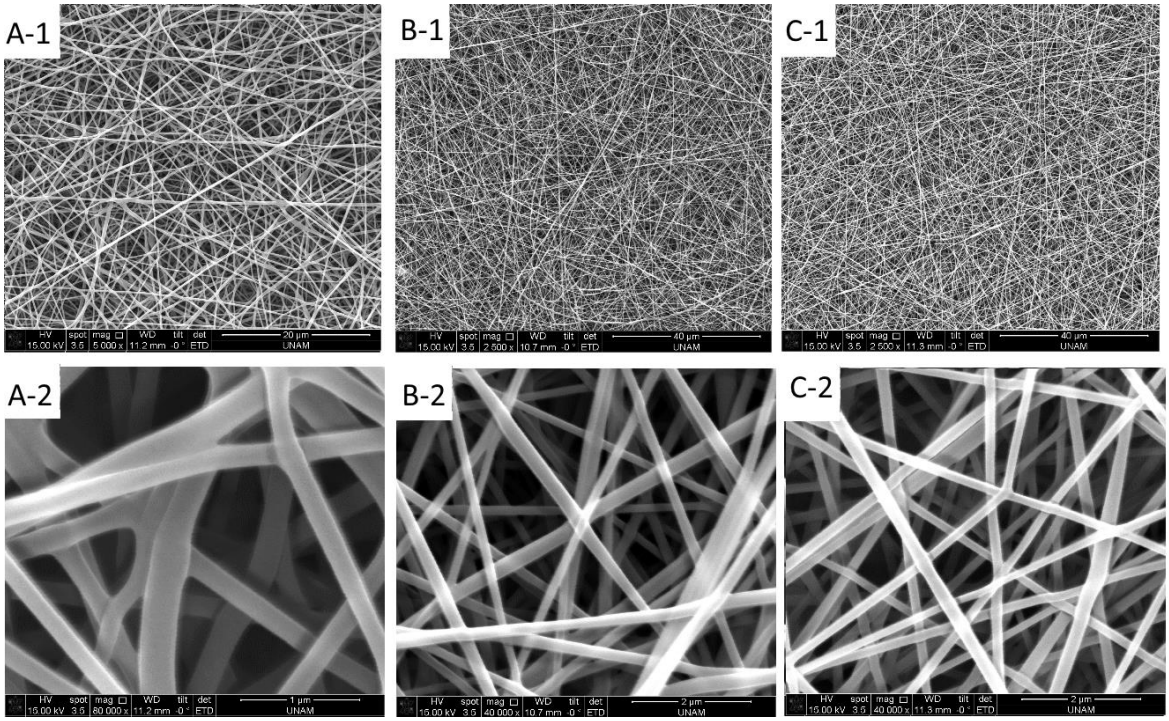

Figure 10:SEM images of DPL-18-4 fibers with different flowrates. A-1 and A-2: DPL-18-4-0.10, B-1 and B-2: DPL-18-4-0.50, C-1 and C-2: DPL-18-4-1.00

3.7. Effect of Distance on PVA/Lignin Fibers

DPL-18-4 solutions were electrospun at 3 different distances (11, 19.5, 25.5 cm). Effect of distance on fiber morphology was observed via SEM images given in Figure 11. To name samples, distance from tip of the needle to collector was added to end of the solution name. Like DPL-18-4-25.5 for DPL-18-4 solution electrospun at distance 25.5 cm. Table 12 shows diameter and experiment condition of samples.

Table 12: Experimental conditions and fiber diameters of DPL-18-4 solution at different distances

Sample	Diameter (nm)	Flow rate (ml/hr)	Voltage (kV)	Distance (cm)
DPL-18-4-25.5	154 ± 19	1.00	25	25.5
DPL-18-4-19.5	120 ± 28	1.00	25	19.5
DPL-18-4-11.0	-	1.00	15	11.00

Diameter of DPL-18-4-11.0 was not calculated since distance was too short for all solvent to evaporate from spinning jet. As a result, wide and thicker fibers stretching over collector were formed [117, 118]. Increasing distance from 11.0 cm to 19.5 cm improved fiber quality drastically. Defect free uniform fibers with 120 nm diameter were produced. Further increase in the distance resulted in formation of bigger fibers. In literature, formation of fibers having better, worser and same morphological properties

with changing distance were reported [118-120]. Increase of the diameter with increasing distance was attributed to less stretching and thinning of the fibers due to less powerful electrical area applied to polymer jet [25].

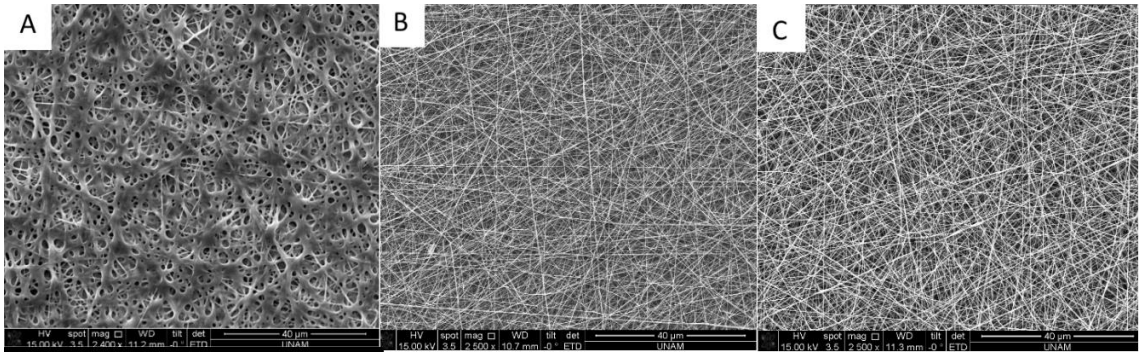

Figure 11:SEM images of PVA/Lignin composite fibers electrospun at different distances. A: DPL-18-4-11.0, B:DPL-18-4-19.5, C:DPL-18-4-25.5

3.8. Antioxidant Activity of PVA/Lignin Fibers and Films

Antioxidant activities of three PVA/Lignin films, six PVA/Lignin nanofibers and PVA and LRF were determined. Pure PVA showed negligible antioxidant activity (0.45 mmol TEAC/kg sample), on the other hand LRF has highest activity 299.29 (mmol TEAC/kg sample). Increasing lignin content increased antioxidant activity for all samples. DPL-18-12 showed highest antioxidant activity among fibers and films, with 131.15 mmol TEAC/kg sample.

Expected antioxidant activities depending on rule of mixtures (ROM) was calculated and compared with antioxidant activity of PVA/Lignin films. All films showed higher antioxidant activities than expected antioxidant activities. PL-4 310%, PL-8 268% and PL-12 had 207% higher antioxidant activity than expected value which indicates that there is a synergistic relationship between PVA and Lignin. According to our knowledge exact mechanism of this synergistic effect is unknown. PVA and lignin forms strong hydrogen bonding between -OH groups, which might prevent lignin to form lignin – lignin interactions and increase antioxidant activity [121, 122]. Increasing lignin content caused to a decrease the difference from expected value. Expected and measured antioxidant activity results are given in Tables 13, 14, 15. and 16.

Table 13:Comparison of theoretical antioxidant activity and measured antioxidant activity

Lignin percentage %	Expected Antioxidant Activity According to ROM (mmol TEAC/kg sample)	Measured Antioxidant Activity (mmol TEAC/kg sample)	Change From Expected Value (%)
4	12.41	50.90	+310
8	24.36	89.72	+268
12	36.31	111.52	+207

* letters within same column represents significant difference ($p<0.05$) between samples.

The antioxidant activity difference of films and fibers containing the same amount of lignin was compared with each other to determine effect of electrospinning on antioxidant activity. Results of the antioxidant activity measurements are given in Table 14 and Figure 13.

Lignin is known as a good free radical scavenger. Hydroxyl and methoxy groups of lignin are able to donate hydrogen and terminate propagation step of oxidation reaction [123].

Every PVA/Lignin composite fiber showed higher antioxidant activity than films containing the same amount of lignin. Highest increase was measured in sample DPL-18-4, 85.84 followed by DPL-16-4, 79.95 which were 68.06 % and 57.07 % higher than antioxidant activities of films. Increasing lignin content above 4% resulted in defected fibers and antioxidant activities of these fibers showed less increase than antioxidant activities of films. Thus, uniform fibers improved antioxidant activity remarkably.

*Table 14: Antioxidant activity of film and fibers containing 4% lignin**

Sample	Antioxidant Activity (mmol TEAC/kg sample)	Change of Antioxidant Activity Compared to Film (%)
PL-4	50.90 ± 2.77^{a}	0.00
DPL-16-4	79.95 ± 3.13^{b}	+57.07
DPL-18-4	85.84 ± 1.63^{b}	+68.06

* Letters within same column represents significant difference ($p<0.05$) between samples.

Fibers produced from solutions having different total solid concentrations (16% and 18%) but same lignin concentration (DPL-16-4 and DPL-18-4, DPL-16-8 and DPL-18-8, DPL-16-12 and DPL-18-12) had similar antioxidant activities. Which indicates that total solid concentration of the electrospinning solution has negligible effect on antioxidant activity of fibers.

*Table 15: Antioxidant activity of film and fibers containing 8% lignin**

Sample	Antioxidant Activity (mmol TEAC/kg sample)	Change of Antioxidant Activity Compared to Film (%)
PL-8	89.72 ± 2.15^{a}	0.00
DPL-16-8	104.83 ± 3.97^{b}	+16.85
DPL-18-8	$97.37 \pm 2.39^{a,b}$	+8.52

* Letters within same column represents significant difference ($p<0.05$) between samples.

*Table 16:Antioxidant activity of film and fibers containing 12% lignin**

Sample	Antioxidant Activity (mmol TEAC/kg sample)	Change of Antioxidant Activity Compared to Film (%)
PL-12	111.52 ± 1.79^{a}	0.00
DPL-16-12	129.95 ± 1.79^{b}	+16.53
DPL-18-12	131.15 ± 3.13^{b}	+17.6

* Letters within same column represents significant difference ($p<0.05$) between samples.

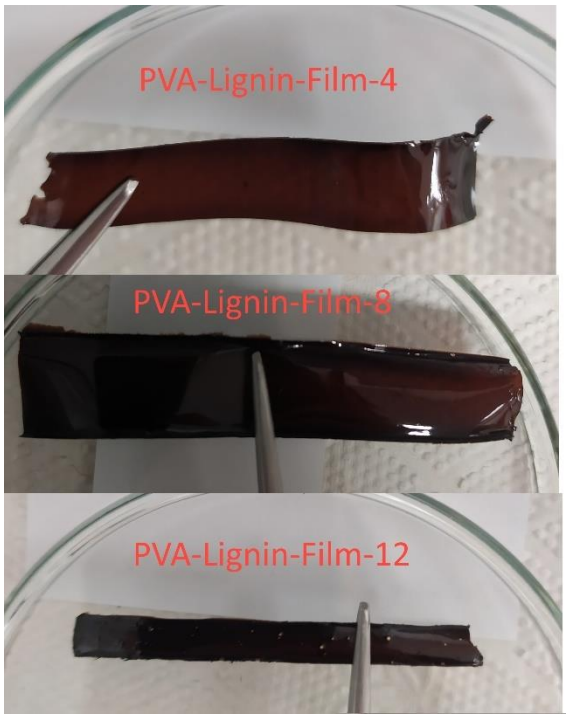

Figure 12: Optic image of PVA/Lignin films

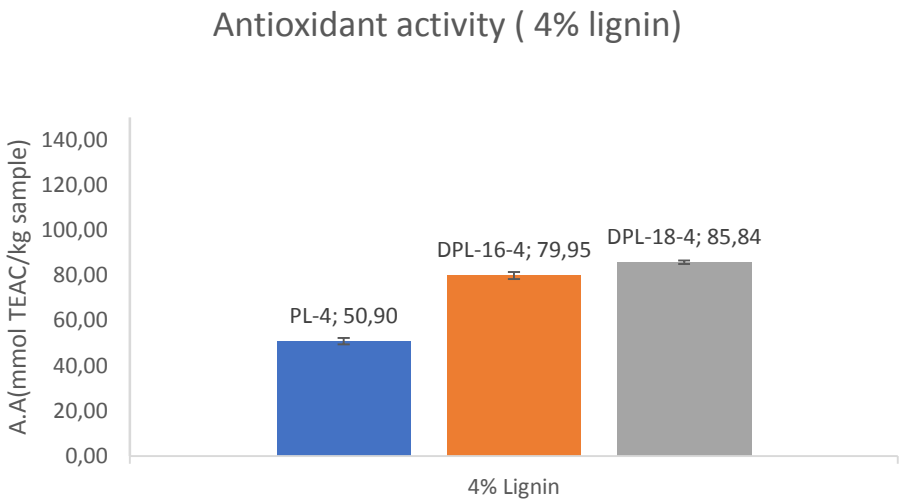
Antioxidant activity (4% lignin)
A.A(mmol TEAC/kg sample)
140,00
120,00
100,00
80,00
60,00
40,00
20,00
0,00
PL-4; 50,90
DPL-16-4; 79,95
DPL-18-4; 85,84
4% Lignin

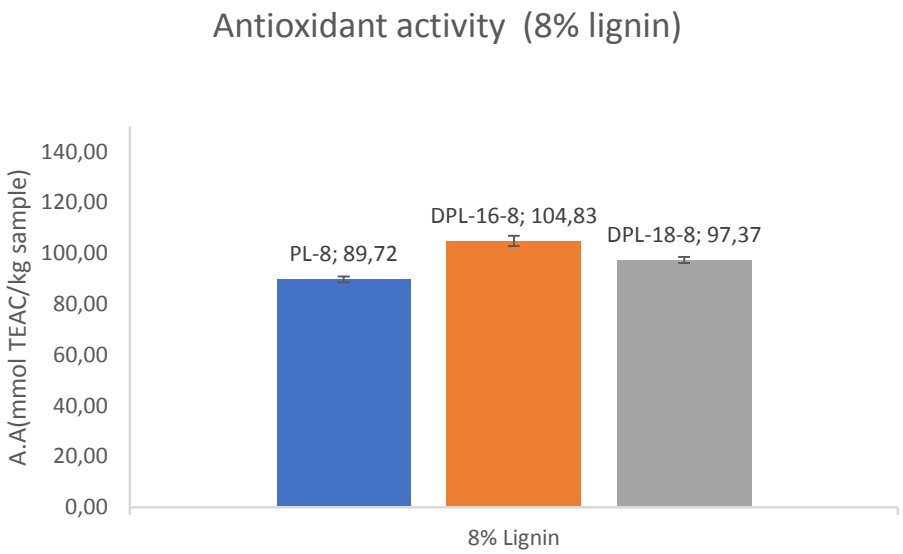
Antioxidant activity (8% lignin)
A.A(mmol TEAC/kg sample)
140,00
120,00
100,00
80,00
60,00
40,00
20,00
0,00
PL-8; 89,72
DPL-16-8; 104,83
DPL-18-8; 97,37
8% Lignin

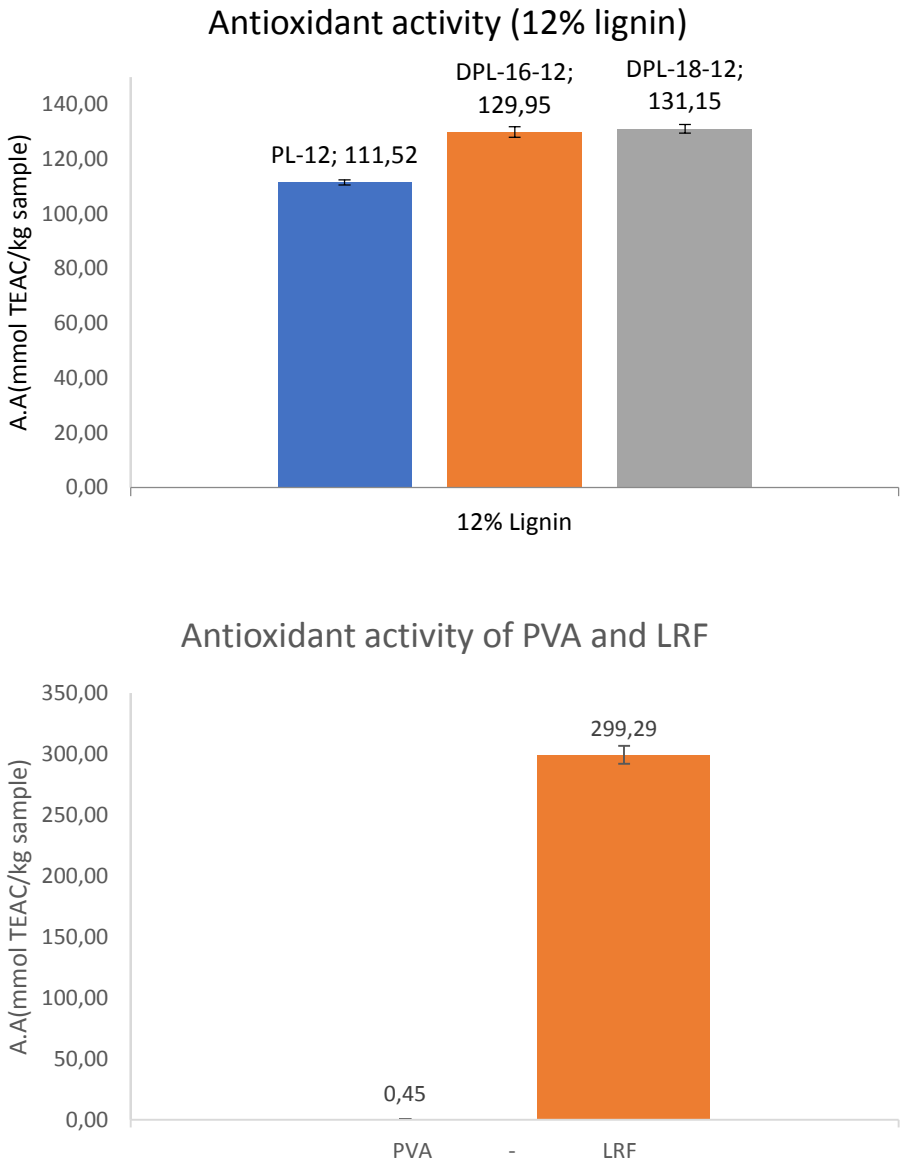

Figure 13:Antioxidant activity of samples

4. CONCLUSION

In this study olive mill solid wastes (OMSW) were pretreated with choline chloride, glycerol, and aluminum chloride hexahydrate ternary deep eutectic solvent (DES). OMSW was delignified successfully and cellulose rich and lignin rich fractions were produced from OMSW. PVA/Lignin composite nano fibers and films were produced from LRF produced from OMSW via DES pretreatment. Antioxidant activities of produced films and fibers were evaluated. Finally effect of electrospinning parameters on fiber morphology was determined.

Effect of aluminum chloride hexahydrate on DES pretreatment was also evaluated. Highest delignification ratio obtained from CGAH-1 was 39.21%. Purity of the obtained LRF was ranged between 83.26 % and 87.21 %. CGAH-3 produced purest lignin. Increasing aluminum chloride hexahydrate concentration of DES were decreased delignification ratio. CGAH-2 had the highest antioxidant activity 437.88 (mmol TEAC/kg sample).

Lignin rich fraction was used to produce PVA/Lignin composite fibers. PVA-Lignin-DMSO solutions containing 16 % and 18 % total solid concentration and 4 % lignin formed uniform nanofibers via electrospinning. Diameter of fibers were ranging between 126 nm – 220 nm. Lignin addition improves fiber morphology of PVA nanofibers up to 4 % above 4% lignin concentration produced fibers had defects such as beads..

Synergistic effect between PVA and lignin in terms of antioxidant activity was observed. Antioxidant activity of PVA/lignin films were up to 310 % higher than calculated antioxidant activity according to ROM. Antioxidant activity of PVA/Lignin films was further increased up to 68 % via formation of nanofibers. Most antioxidant fiber produced in this study showed 131.15 (mmol TEAC/kg sample) antioxidant activity. Results indicated that uniformity of the nanofibers has positive effect on antioxidant activity.

Factors affecting electrospinning of PVA/Lignin mixture were investigated. Effect of total solid concentration of electrospinning solution, electrospinning distance and flow rate were investigated and their effect on fiber morphology was demonstrated. Total

solid concentration of solutions did not affect fiber morphology. Optimum electrospinning conditions were observed at 19.5 cm distance and at 1.00 mL/hr flow rate.

These results show that PVA/Lignin nanofibers might be produced from DES pretreated OMSW, and these nanofibers may use as a food packaging material. More detailed study needed to increase efficiency of the overall system. To increase delignification higher temperature and time combinations might be used during pretreatment. Production of fibers with higher lignin concentration, producing purer lignin at pretreatment might improve antioxidant activity of fibers.

REFERENCES

1. Ubando, A.T., C.B. Felix, and W.H. Chen, Biorefineries in circular bioeconomy: A comprehensive review. Bioresource Technology, 2020. **299**.
2. Özdenkçi, K., et al., A novel biorefinery integration concept for lignocellulosic biomass. Energy Conversion and Management, 2017. **149**: p. 974-987.
3. Sawatdeenarunat, C., et al., Decentralized biorefinery for lignocellulosic biomass: Integrating anaerobic digestion with thermochemical conversion. Bioresource Technology, 2018. **250**: p. 140-147.
4. Bastidas-Oyanedel, J.R. and J.E. Schmidt, Increasing profits in food waste biorefinery-a techno-economic analysis. Energies, 2018. **11**.
5. Dahiya, S., et al., Food waste biorefinery: Sustainable strategy for circular bioeconomy. Bioresource Technology, 2018. **248**: p. 2-12.
6. Esteban, J. and M. Ladero, Food waste as a source of value-added chemicals and materials: a biorefinery perspective. International Journal of Food Science and Technology, 2018. **53**: p. 1095-1108.
7. Li, J., et al., Characterization of food gels prepared from the water extract of fish (Cyprinus carpio L.) scales: From molecular components to sensory attributes. Food Hydrocolloids, 2021. **112**.
8. De Bhowmick, G., A.K. Sarmah, and R. Sen, Zero-waste algal biorefinery for bioenergy and biochar: A green leap towards achieving energy and environmental sustainability. Science of the Total Environment, 2019. **650**: p. 2467-2482.
9. Nimmanterdwong, P., B. Chalermsinsuwan, and P. Piumsomboon, Prediction of lignocellulosic biomass structural components from ultimate/proximate analysis. Energy, 2021. **222**.
10. Singhvi, M.S., S. Chaudhari, and D.V. Gokhale, Lignocellulose processing: A current challenge. RSC Advances, 2014. **4**: p. 8271-8277.
11. Heinze, T., O.A.E. Seoud, and A. Koschella, Cellulose Derivatives: Synthesis, Structure, and Properties. 2018: Springer International Publishing.
12. Hu, F. and A. Ragauskas, Pretreatment and Lignocellulosic Chemistry. Bioenergy Research, 2012. **5**: p. 1043-1066.
13. George, J. and S.N. Sabapathi, Cellulose nanocrystals: synthesis, functional properties, and applications. Nanotechnol Sci Appl, 2015. **8**: p. 45-54.
14. Heinze, T., T. Liebert, and A. Koschella, Esterification of Polysaccharides Journal of the American Chemical Society, 2007. **129**(7): p. 2195-2196.
15. Huang, J., S. Fu, and L. Gan, Lignin Chemistry and Applications, in Lignin Chemistry and Applications. 2019, Elsevier. p. 25-50.
16. Harmsen, P.F.H., et al., Literature review of physical and chemical pretreatment processes for lignocellulosic biomass. 2010, Wageningen UR - Food & Biobased Research: Wageningen.
17. Lou, R., et al., Facile Extraction of Wheat Straw by Deep Eutectic Solvent (DES) to Produce Lignin Nanoparticles. ACS Sustainable Chemistry and Engineering, 2019. **7**: p. 10248-10256.
18. Harun, S. and S. Geok, Effect of Sodium Hydroxide Pretreatment on Rice Straw Composition. Indian Journal of Science and Technology, 2016. **9**.

19. Solarte-Toro, J.C., et al., Acid pretreatment of lignocellulosic biomass for energy vectors production: A review focused on operational conditions and techno-economic assessment for bioethanol production. Renewable and Sustainable Energy Reviews, 2019. **107**: p. 587-601.
20. Zhang, J., et al., The effects of four different pretreatments on enzymatic hydrolysis of sweet sorghum bagasse. Bioresource Technology, 2011. **102**: p. 4585-4589.
21. Shuai, L., et al., Comparative study of SPORL and dilute-acid pretreatments of spruce for cellulosic ethanol production. 2010(1873-2976 (Electronic)).
22. Carvalheiro, F., L. Duarte, and F. Gírio, Hemicellulose biorefineries: A review on biomass pretreatments. Journal of scientific and industrial research, 2008. **67**: p. 849.
23. Kang, Y., et al., Lignocellulosic nanofiber prepared by alkali treatment and electrospinning using ionic liquid. Fibers and Polymers, 2013. **14**: p. 530-536.
24. Bauer, A., et al., Steam explosion pretreatment for enhancing biogas production of late harvested hay. Bioresource Technology, 2014. **166**: p. 403-410.
25. Chandra, R.P., et al., The influence of lignin on steam pretreatment and mechanical pulping of poplar to achieve high sugar recovery and ease of enzymatic hydrolysis. Bioresource Technology, 2016. **199**: p. 135-141.
26. Mokomele, T., et al., Ethanol production potential from AFEX™ and steam-exploded sugarcane residues for sugarcane biorefineries. (1754-6834 (Print)).
27. Nielsen, F., et al., The effect of mixed agricultural feedstocks on steam pretreatment, enzymatic hydrolysis, and cofermentation in the lignocellulose-to-ethanol process. Biomass Conversion and Biorefinery, 2020. **10**(2): p. 253-266.
28. Borrega, M., K. Nieminen, and H. Sixta, Degradation kinetics of the main carbohydrates in birch wood during hot water extraction in a batch reactor at elevated temperatures. Bioresource Technology, 2011. **102**(22): p. 10724-10732.
29. Szczodrak, J., et al., Intensification of oak sawdust enzymatic hydrolysis by chemical or hydrothermal pretreatment. (0006-3592 (Print)).
30. Van Walsum, G.P., et al., Conversion of lignocellulosics pretreated with liquid hot water to ethanol. Applied Biochemistry and Biotechnology - Part A Enzyme Engineering and Biotechnology, 1996. **57-58**: p. 157-170.
31. Melro, E., et al., A brief overview on lignin dissolution. Journal of Molecular Liquids, 2018. **265**: p. 578-584.
32. Galbe, M. and O. Wallberg, Pretreatment for biorefineries: a review of common methods for efficient utilisation of lignocellulosic materials. Biotechnol Biofuels, 2019. **12**: p. 294.
33. Borand, M.N. and F. Karaosmanoğlu, Effects of organosolv pretreatment conditions for lignocellulosic biomass in biorefinery applications: A review. Journal of Renewable and Sustainable Energy, 2018. **10**.
34. Yoo, C.G., Y. Pu, and A.J. Ragauskas, Ionic liquids: Promising green solvents for lignocellulosic biomass utilization. Current Opinion in Green and Sustainable Chemistry, 2017. **5**: p. 5-11.
35. Hossain, M.M. and L. Aldous, Ionic Liquids for Lignin Processing: Dissolution, Isolation, and Conversion. Australian Journal of Chemistry, 2012. **65**(11).
36. Casas, A., et al., Relation between differential solubility of cellulose and lignin in ionic liquids and activity coefficients. RSC Advances, 2013. **3**(10).
37. Earle, M.J. and K.R. Seddon, Ionic liquids. Green solvents for the future. Pure and Applied Chemistry, 2000. **72**(7): p. 1391-1398.
38. Seddon, K.R., A taste of the future. Nature Materials, 2003. **2**(6): p. 363-365.

39. Xiong, D., et al., Recovery of ionic liquids with aqueous two-phase systems induced by carbon dioxide. 2012(1864-564X (Electronic)).
40. Abbott, A.P., et al., Novel solvent properties of choline chloride/urea mixtures. Chem Commun (Camb), 2003(1): p. 70-1.
41. Wang, Z.K., et al., Lewis Acid-Facilitated Deep Eutectic Solvent (DES) Pretreatment for Producing High-Purity and Antioxidative Lignin. ACS Sustainable Chemistry and Engineering, 2020. **8**: p. 1050-1057.
42. Ragauskas, A.J., et al., Lignin valorization: improving lignin processing in the biorefinery. (1095-9203 (Electronic)).
43. Liu, Y., et al., Efficient Cleavage of Lignin–Carbohydrate Complexes and Ultrafast Extraction of Lignin Oligomers from Wood Biomass by Microwave-Assisted Treatment with Deep Eutectic Solvent. ChemSusChem, 2017. **10**(8): p. 1692-1700.
44. Xie, Y., et al., Solubilities of CO2, CH4, H2, CO and N2 in choline chloride/urea. Green Energy and Environment, 2016. **1**: p. 195-200.
45. Jeong, K.M., et al., Highly efficient extraction of anthocyanins from grape skin using deep eutectic solvents as green and tunable media. Archives of Pharmacal Research, 2015. **38**: p. 2143-2152.
46. Abbott, A.P., et al., Selective extraction of metals from mixed oxide matrixes using choline-based ionic liquids. Inorganic Chemistry, 2005. **44**: p. 6497-6499.
47. Coulembier, O., et al., Synthesis of poly(l-lactide) and gradient copolymers from a l-lactide/trimethylene carbonate eutectic melt. Chemical Science, 2012. **3**: p. 723-726.
48. Zhang, Q., et al., Deep eutectic solvents: Syntheses, properties and applications. Chemical Society Reviews, 2012. **41**: p. 7108-7146.
49. Imperato, G., et al., Low melting sugar-urea-salt mixtures as solvents for organic reactions - Estimation of polarity and use in catalysis. Green Chemistry, 2006. **8**: p. 1051-1055.
50. Zhang, C.W., S.Q. Xia, and P.S. Ma, Facile pretreatment of lignocellulosic biomass using deep eutectic solvents. Bioresource Technology, 2016. **219**: p. 1-5.
51. Cinlar, B., T. Wang, and B.H. Shanks, Kinetics of monosaccharide conversion in the presence of homogeneous Bronsted acids. Applied Catalysis A: General, 2013. **450**: p. 237-242.
52. Ji, Q., et al., Efficient removal of lignin from vegetable wastes by ultrasonic and microwave-assisted treatment with ternary deep eutectic solvent. Industrial Crops and Products, 2020. **149**: p. 112357.
53. IOC, Huiles D ' Olive - Olive Oils. International Olive Oil Council, 2018: p. 2018.
54. McNamara, C.J., et al., Bioremediation of olive mill wastewater. International Biodeterioration & Biodegradation, 2008. **61**(2): p. 127-134.
55. IOC, Olive oil production data. 2020.
56. Galanakis, C.M., Olive Mill Waste Recent Advances for Sustainable Management Preface. Olive Mill Waste: Recent Advances for Sustainable Management, 2017: p. Xv-Xvi.
57. Tian, D., et al., Acidic deep eutectic solvents pretreatment for selective lignocellulosic biomass fractionation with enhanced cellulose reactivity. International Journal of Biological Macromolecules, 2020. **142**: p. 288-297.
58. Kim, K.H., et al., Biomass pretreatment using deep eutectic solvents from lignin derived phenols. Green Chemistry, 2018. **20**(4): p. 809-815.

59. Chen, Z., W.D. Reznicek, and C. Wan, Deep eutectic solvent pretreatment enabling full utilization of switchgrass. Bioresource Technology, 2018. **263**: p. 40-48.
60. Shen, X.-j., et al., Facile fractionation of lignocelluloses by biomass-derived deep eutectic solvent (DES) pretreatment for cellulose enzymatic hydrolysis and lignin valorization. 2019: p. 275-283.
61. Guo, Z., et al., Short-time deep eutectic solvent pretreatment for enhanced enzymatic sacchari fi cation and lignin. 2019: p. 3099-3108.
62. Chen, Z., W.A. Jacoby, and C. Wan, Ternary deep eutectic solvents for effective biomass deconstruction at high solids and low enzyme loadings. Bioresource Technology, 2019. **279**: p. 281-286.
63. Ahmad, W.-l.L., et al., Alkaline deep eutectic solvent : a novel green solvent for lignocellulose pulping. Cellulose, 2019. **26**: p. 4085-4098.
64. Rahmanian, N., S.M. Jafari, and C.M. Galanakis, Recovery and Removal of Phenolic Compounds from Olive Mill Wastewater. Journal of the American Oil Chemists' Society, 2014. **91**(1): p. 1-18.
65. Montiel Jarillo, G., et al., Towards PHA production from wastes: The bioconversion potential of different activated sludge and food industry wastes into VFAs through acidogenic fermentation. 2021.
66. Branciari, R., et al., Dietary Supplementation with Olive Mill Wastewater in Dairy Sheep: Evaluation of Cheese Characteristics and Presence of Bioactive Molecules. Animals (Basel), 2020. **10**(11).
67. Romeo, R., et al., Impact of Stability of Enriched Oil with Phenolic Extract from Olive Mill Wastewaters. Foods, 2020. **9**(7).
68. Tapia-Quiros, P., et al., Olive Mill and Winery Wastes as Viable Sources of Bioactive Compounds: A Study on Polyphenols Recovery. Antioxidants (Basel), 2020. **9**(11).
69. Ricelli, A., et al., Antioxidant and Biological Activities of Hydroxytyrosol and Homovanillic Alcohol Obtained from Olive Mill Wastewaters of Extra-Virgin Olive Oil Production. J Agric Food Chem, 2020. **68**(52): p. 15428-15439.
70. El Kassis, E., et al., Assessment of olive pomace wastes as flame retardants. Journal of Applied Polymer Science, 2019. **137**(1).
71. Sisti, L., et al., Olive Mill Wastewater Valorization in Multifunctional Biopolymer Composites for Antibacterial Packaging Application. Int J Mol Sci, 2019. **20**(10).
72. Roila, R., et al., Antimicrobial and anti-biofilm activity of olive oil by-products against Campylobacter spp. isolated from chicken meat [pdf]. Acta Scientiarum Polonorum Technologia Alimentaria, 2019. **18**(1): p. 43-52.
73. Difonzo, G., et al., Functional compounds from olive pomace to obtain high-added value foods – a review. Journal of the Science of Food and Agriculture, 2021. **101**(1): p. 15-26.
74. Athanasiadis, V., et al., Highly Efficient Extraction of Antioxidant Polyphenols from Olea europaea Leaves Using an Eco-friendly Glycerol/Glycine Deep Eutectic Solvent. Waste and Biomass Valorization, 2018. **9**: p. 1985-1992.
75. Chanioti, S. and C. Tzia, Extraction of phenolic compounds from olive pomace by using natural deep eutectic solvents and innovative extraction techniques. Innovative Food Science and Emerging Technologies, 2018. **48**: p. 228-239.
76. Gu, T., et al., Deep eutectic solvents as novel extraction media for phenolic compounds from model oil. Chemical Communications, 2014. **50**: p. 11749-11752.

77. de Jong, E. and G. Jungmeier, Chapter 1 - Biorefinery Concepts in Comparison to Petrochemical Refineries, in Industrial Biorefineries & White Biotechnology, A. Pandey, et al., Editors. 2015, Elsevier: Amsterdam. p. 3-33.
78. Agarwal, S., J.H. Wendorff, and A. Greiner, Use of electrospinning technique for biomedical applications. Polymer, 2008. **49**(26): p. 5603-5621.
79. Xue, J., et al., Electrospinning and Electrospun Nanofibers: Methods, Materials, and Applications. Chemical Reviews, 2019. **119**(8): p. 5298-5415.
80. Inovenso. Difference Between ElectroSpinning and ElectroSpraying. 2021; Available from: https://www.inovenso.com/electrospinning-and-electrospraying/.
81. Cho, M., et al., High performance electrospun carbon nanofiber mats derived from flax lignin. Industrial Crops and Products, 2020. **155**.
82. Fontes, M.R.V., et al., Thermal stability, hydrophobicity and antioxidant potential of ultrafine poly (lactic acid)/rice husk lignin fibers. Brazilian Journal of Chemical Engineering, 2021. **38**(1): p. 133-144.
83. Zhang, X., et al., Influence of Lignin units on the properties of Lignin/

PAN

-derived carbon fibers. Journal of Applied Polymer Science, 2020. **137**(42).
84. Ogale, A., M. Zhang, and J. Jin, Recent advances in carbon fibers derived from biobased precursors. Journal of Applied Polymer Science, 2016. **133**.
85. Wei, J., et al., Green Carbon Nanofiber Networks for Advanced Energy Storage. ACS Applied Energy Materials, 2020. **3**(4): p. 3530-3540.
86. Camire, A., et al., Development of electrospun lignin nanofibers for the adsorption of pharmaceutical contaminants in wastewater. Environ Sci Pollut Res Int, 2020. **27**(4): p. 3560-3573.
87. Zhang, W., et al., Electrospun lignin-based composite nanofiber membrane as high-performance absorbent for water purification. Int J Biol Macromol, 2019. **141**: p. 747-755.
88. Liengprayoon, S., et al., Investigation of the potential for utilization of sugarcane bagasse lignin for carbon fiber production: Thailand case study. SN Applied Sciences, 2019. **1**(10).
89. Perera Jayawickramage, R.A., K.J. Balkus, and J.P. Ferraris, Binder free carbon nanofiber electrodes derived from polyacrylonitrile-lignin blends for high performance supercapacitors. Nanotechnology, 2019. **30**(35): p. 355402.
90. Perera Jayawickramage, R.A. and J.P. Ferraris, High performance supercapacitors using lignin based electrospun carbon nanofiber electrodes in ionic liquid electrolytes. Nanotechnology, 2019. **30**(15): p. 155402.
91. Hong, J.H., et al., Eco-friendly lignin nanofiber mat for protection of wood against attacks by environmentally hazardous fungi. Polymer Testing, 2019. **74**: p. 113-118.
92. Schlee, P., et al., Free-standing supercapacitors from Kraft lignin nanofibers with remarkable volumetric energy density. Chem Sci, 2019. **10**(10): p. 2980-2988.
93. Ma, X., A.L. Smirnova, and H. Fong, Flexible lignin-derived carbon nanofiber substrates functionalized with iron (III) oxide nanoparticles as lithium-ion battery anodes. Materials Science and Engineering: B, 2019. **241**: p. 100-104.
94. Vivo-Vilches, J.F., et al., Lignin-Based Carbon Nanofibers as Electrodes for Vanadium Redox Couple Electrochemistry. Nanomaterials (Basel), 2019. **9**(1).

95. Lee, E., Y. Song, and S. Lee, Crosslinking of lignin/poly(vinyl alcohol) nanocomposite fiber webs and their antimicrobial and ultraviolet-protective properties. Textile Research Journal, 2017. **89**(1): p. 3-12.
96. Dalton, N., et al., Thermoelectric properties of electrospun carbon nanofibres derived from lignin. Int J Biol Macromol, 2019. **121**: p. 472-479.
97. Salas, C., et al., Synthesis of soy protein-lignin nanofibers by solution electrospinning. Reactive and Functional Polymers, 2014. **85**: p. 221-227.
98. Helrich, K., Official methods of analysis of the AOAC. Vol. 1. 1990: Association of Offical analytical Cehmists
99. Baeta-Hall, L., et al., Bio-degradation of olive oil husks in composting aerated piles. Bioresour Technol, 2005. **96**(1): p. 69-78.
100. Serpen, A., et al., Direct measurement of the total antioxidant capacity of cereal products. Journal of Cereal Science, 2008. **48**(3): p. 816-820.
101. Sluiter, A., et al., Determination of structural carbohydrates and lignin in biomass. Laboratory analytical procedure, 2008. **1617**(1): p. 1-16.
102. Tan, Y.T., G.C. Ngoh, and A.S.M. Chua, Effect of functional groups in acid constituent of deep eutectic solvent for extraction of reactive lignin. Bioresource Technology, 2019. **281**: p. 359-366.
103. Ouazzane, H., et al., Olive Mill Solid Waste Characterization and Recycling opportunities : A review. Journal of Materials and Environmental Sciences, 2017. **8**: p. 2632-2650.
104. Ducom, G., et al., Comparative analyses of three olive mill solid residues from different countries and processes for energy recovery by gasification. Renewable Energy, 2020. **145**: p. 180-189.
105. Yu, H., Multiple hydrogen bond coordination in three-constituent deep eutectic solvents enhances lignin fractionation from biomass. 2018. **20**.
106. Bichot, A., et al., Understanding biomass recalcitrance in grasses for their efficient utilization as biorefinery feedstock. Reviews in Environmental Science and Bio/Technology, 2018. **17**(4): p. 707-748.
107. Alvarez-Vasco, C., et al., Unique low-molecular-weight lignin with high purity extracted from wood by deep eutectic solvents (DES): a source of lignin for valorization. Green Chemistry, 2016. **18**(19): p. 5133-5141.
108. Yu, Z., et al., Effect of lignin chemistry on the enzymatic hydrolysis of woody biomass. (1864-564X (Electronic)).
109. Herbaut, M., et al., Multimodal analysis of pretreated biomass species highlights generic markers of lignocellulose recalcitrance. (1754-6834 (Print)).
110. Guo, Y., et al., Transparent Cellulose/Technical Lignin Composite Films for Advanced Packaging. Polymers (Basel), 2019. **11**(9).
111. Cequier, E., et al., Extraction and characterization of lignin from olive pomace: a comparison study among ionic liquid, sulfuric acid, and alkaline treatments. Biomass Conversion and Biorefinery, 2019. **9**(2): p. 241-252.
112. Chua, K.Y., et al., Cellulose-based polymer electrolyte derived from waste coconut husk: residual lignin as a natural plasticizer. Journal of Polymer Research, 2020. **27**(5).
113. Adapa, et al., Quantitative analysis of lignocellulosic components of non-treated and steam exploded Barley, Canola, Oat and wheat straw using Fourier Transform Infrared Spectroscopy. Journal of Agricultural Science and Technology, 2011. **B1**: p. 177-188.
114. Rwei, S.-P. and C.-C. Huang, Electrospinning PVA solution-rheology and morphology analyses. Fibers and Polymers, 2012. **13**(1): p. 44-50.

115. Zargham, S., et al., The Effect of Flow Rate on Morphology and Deposition Area of Electrospun Nylon 6 Nanofiber. Journal of Engineered Fibers and Fabrics, 2012. **7**: p. 42-49.
116. Haider, A., S. Haider, and I.-K. Kang, A comprehensive review summarizing the effect of electrospinning parameters and potential applications of nanofibers in biomedical and biotechnology. Arabian Journal of Chemistry, 2018. **11**(8): p. 1165-1188.
117. Abbas, L., A. Jabur, and S. Muhi, Effects of High Voltage and Flow Rate Parameters on Nanofibers Diameter Synthesis by Electrospinning Technique. Journal of Physical Science and Application, 2016. **6**: p. 122-130.
118. Gupta, D., M. Jassal, and A.K. Agrawal, Atypical rheology and spinning behavior of poly(vinyl alcohol) in a nonaqueous solvent. Polymer Journal, 2019. **51**(9): p. 883-894.
119. Matabola, K.P. and R.M. Moutloali, The influence of electrospinning parameters on the morphology and diameter of poly(vinyledene fluoride) nanofibers- effect of sodium chloride. Journal of Materials Science, 2013. **48**(16): p. 5475-5482.
120. Salehhudin, H., et al., Multiple-jet electrospinning methods for nanofiber processing: A review. Materials and Manufacturing Processes, 2017. **33**: p. 479-498.
121. Yang, W., et al., Antioxidant and antibacterial lignin nanoparticles in polyvinyl alcohol/chitosan films for active packaging. Industrial Crops and Products, 2016. **94**: p. 800-811.
122. Hu, X.-Q., et al., From waste to functional additives: thermal stabilization and toughening of PVA with lignin. RSC Advances, 2016. **6**(17): p. 13797-13802.
123. Kai, D., et al., Towards lignin-based functional materials in a sustainable world. Green Chemistry, 2016. **18**(5): p. 1175-1200.